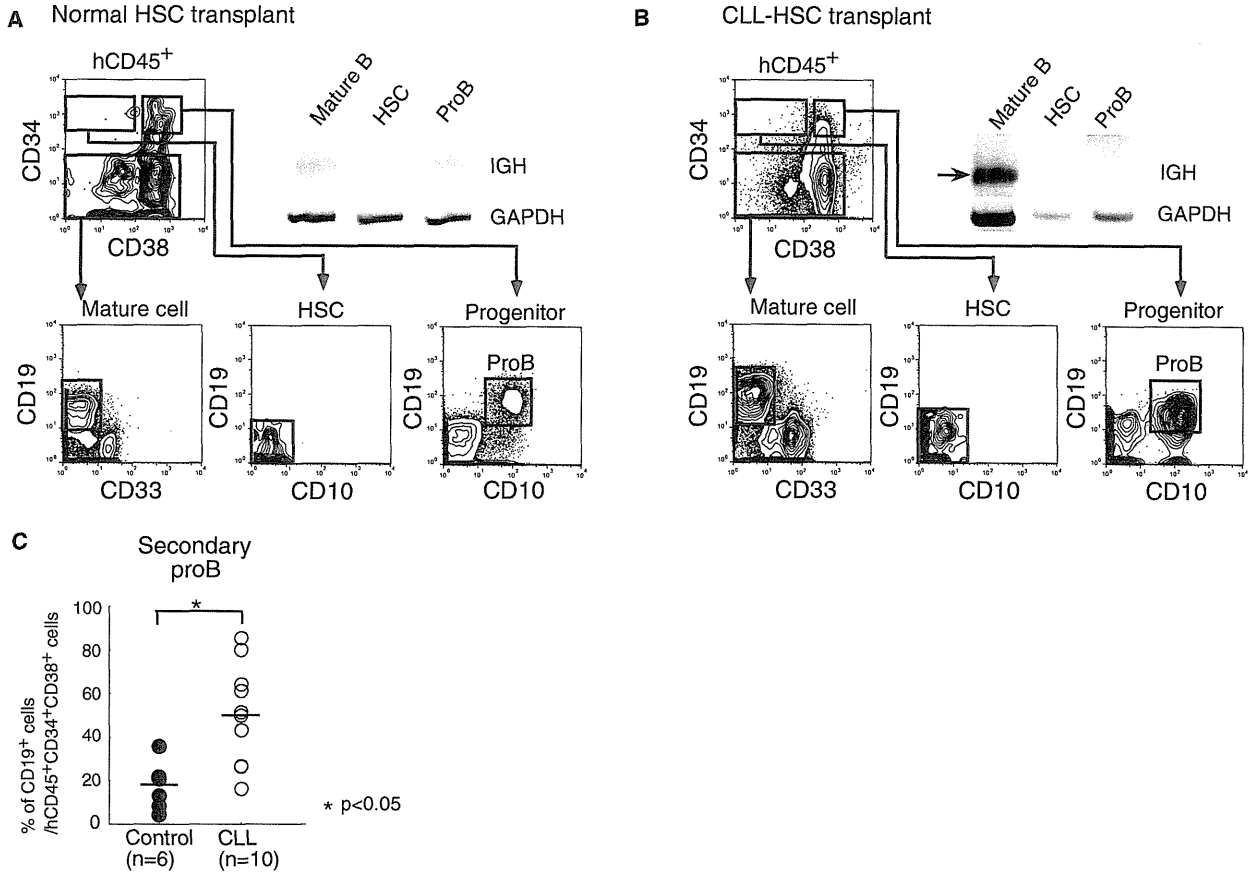

Figure 2. The Bone Marrow Cell Analysis in Mice Transplanted with the CD34$^+$CD38$^-$ HSC Population Purified from Normal Controls and Patients with CLL

(A and B) IGH rearrangement status of HSC, proB, and B cell fractions and in the bone marrow of mice transplanted with normal HSCs (A) and CLL-HSCs (B). In all analysis, secondary HSCs and proB cells showed germline and polyclonal rearrangement of IGH genes, respectively. However, secondary mature B cells had clonal IGH only in mice reconstituted with CLL-HSCs but not in those transplanted with normal HSCs. These results suggest that B cell clones derived from CLL-HSCs were selected in vivo.

(C) Frequencies of proB cells in the bone marrow of mice transplanted with CLL-HSCs and normal HSCs. A representative xenogeneic transplantation result of CD19$^+$ CLL cells is shown in **Figure S1**.

(**Table 1**). These CD5$^+$ B cells derived from CLL-HSCs expressed surface IgM, CD20, and CD23 (**Figure 3**C) but lacked CD10, like original CLL cells in patients.

CLL-HSC-Derived B Cell Clones Had IGH-VDJ Combination Independent of the Original CLL Clones, and Used Preferentially the VH1, VH3, and VH4 Genes

IGH rearrangement status of CLL-HSC-derived B cells was then tested by PCR analysis. In the mouse bone marrow transplanted with normal HSCs (**Figure 2**A), secondary CD34$^+$CD38$^-$ HSCs did not rearrange IGH, and both proB and CD5$^-$ mature B cells had polyclonal rearrangement, indicating that control HSCs normally develop polyclonal B cells in this system. Similarly, in mice reconstituted with CLL-HSCs, secondary HSCs retained the germline, and the expanded proB cell population displayed polyclonal IGH rearrangement (**Figure 2**B). However, to our surprise, mature B cell progeny appeared to have monoclonal or oligoclonal IGH rearrangement, suggesting that clonal selection of B cells occurred even in xenogeneic recipients (Figures 2B and 3B).

We then analyzed the usage of the VDJ genes in B cell progeny to evaluate clonal relationships between patients' original CLL cells and B cell clones developed in mice from CLL-HSCs. When we found clonal bands in the IGH rearrangement analysis, we evaluated the frequency of B cell clones with specific VDJs by TA cloning of the IGH gene PCR products (**Landgren et al., 2009**). The PCR products were ligated into the vector, transformed in *Escherichia coli*, picked up randomly ~35 colonies per CD5$^+$ or CD5$^-$ B cell samples on average, and they were sequenced to confirm the clonality of BCRs. This analysis was performed in 25 mice reconstituted with 16 patients' CLL-HSCs (**Table S2**).

Figure 3 shows the representative VDJ recombination analysis of B cell progeny in mice reconstituted with normal HSCs from healthy donors (**Figure 3**A), or with CLL-HSCs from patients 5, 7, 8, and 13 (**Figure 3**B). Strikingly, in mice transplanted with CLL-HSCs from these patients, both CD5$^+$ and CD5$^-$ B cells

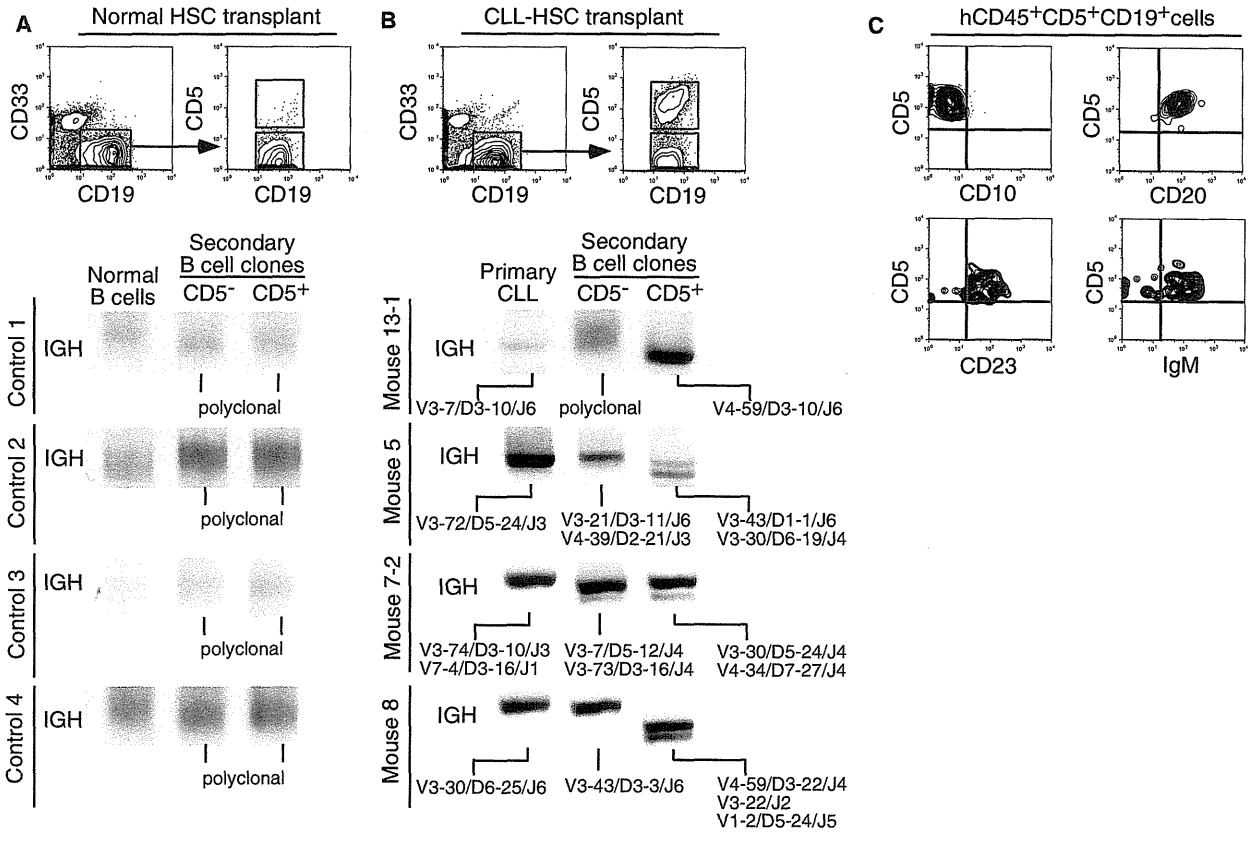

Figure 3. CLL-HSCs Give Rise to Monoclonal or Oligoclonal B Cells with CLL-like Phenotype after Xenogeneic Transplantation

(A) FACS and IGH rearrangement analysis of mice transplanted with normal HSCs. $CD5^+$ B cells were rare, and both $CD5^+CD19^+$ and $CD5^-CD19^+$ B cell fractions displayed polyclonal IGH rearrangement.

(B) FACS and IGH rearrangement analysis of mice transplanted with CLL-HSCs. Development of $CD5^+CD19^+$ B cells was frequently seen in these mice (as summarized in **Table 1**). In mouse 13-1, $CD5^-$ B cells were polyclonal, but $CD5^+$ B cells were monoclonal. In other mice shown here, both $CD5^-$ and $CD5^+$ B cells are composed of one to three B cell clones. The B cell clones developed in mice always had VDJ genes different from those of the original CLL cells and, therefore, were independent of the original patients' CLL clone. VH gene usage and similarity of CDR3 amino acid sequences of these independent B cell clones are shown in **Figure S2**.

(C) The CLL-HSC-derived B cell clones expressed CD20, CD23, and IgM. Representative data are shown.

were developed, and each of them was composed of one to three B cell clones. Importantly, these B cell clones developed in recipients possessed the VDJ combinations different from those used in CLL clones in original patients (**Figure 3**B). In summary, $CD5^+$ B cells were developed in 14 out of 25 mice transplanted with CLL-HSCs, and these $CD5^+$ B cells consisted always of mono- or oligo-clones (**Table 1**). Clonal B cell populations were also found in $CD5^-$ B cell progeny in 16 out of 25 mice transplanted with CLL-HSCs (**Table 1**). As a result, in all patients analyzed, mice transplanted with CLL-HSCs developed B cell clones either of $CD5^+$ phenotype, $CD5^-$ phenotype, or both (**Table 1**), whose VDJs were always independent of those in original CLL cells (**Table S2**).

Furthermore, when we transplanted CLL-HSCs from single patients (patients 7, 9, 10, and 13) into more than two mice simultaneously, the B cell progeny of each mouse was again composed of independent clones with different VDJ recombination (**Table S2**). Representative data of patient 10 are shown in **Figure 4**A. These data suggest that the clonal selection occurs within polyclonal B cell progeny in each recipient somewhat in a stochastic manner.

Table S2 summarized VDJ recombination and amino acid sequences of CDR3 in CLL-HSC-derived B cell clones. It has been shown that de novo CLL cells preferentially used VH1, VH3, and VH4 for IGH rearrangement (**Chiorazzi and Ferrarini, 2003; Fais et al., 1998**). Interestingly, frequency of VH1, VH3, and VH4 usage is higher in B cell clones derived from CLL-HSCs (48 out of 50 clones), as compared to polyclonal B cells developed from normal HSCs (197 out of 233 clones) (**Figure S2**). The difference was statistically significant on Fisher's exact test ($p < 0.05$).

The status of SHM was also evaluated. Sequencing results with less than 98% germline identity were judged as mutated, whereas those with >98% germline identity were regarded as unmutated (**Damle et al., 1999; Hamblin et al., 1999**). The majority (45 out of 50) of B cell clones after transplantation

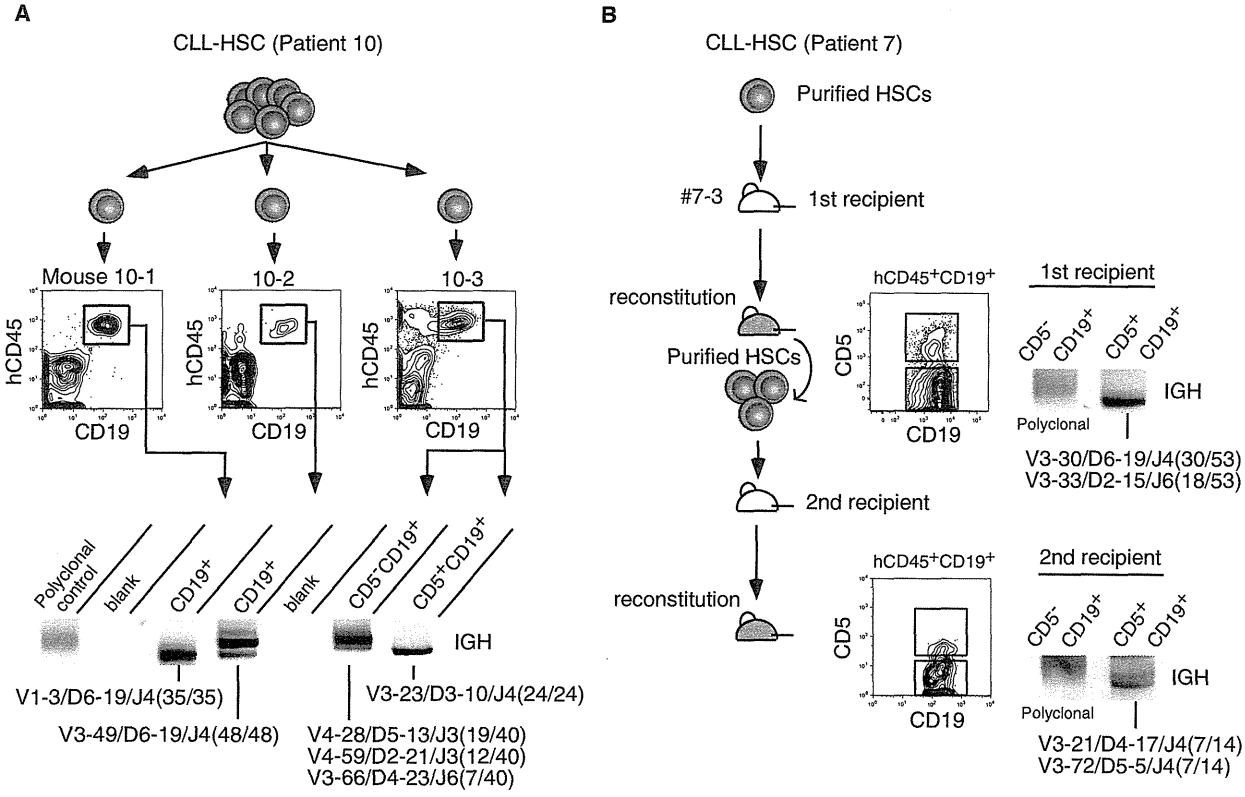

Figure 4. CLL-HSCs Are Capable of Self-renewal, and Their B Cell Progeny Is Clonally Selected in Xenogeneic Recipients

(A) CLL-HSCs from patient 10 were purified and transplanted into three recipients simultaneously. All recipients developed monoclonal or oligoclonal B cell clones. Note that the B cell clones of each mouse were independent and used different VDJ genes.

(B) HSCs were harvested from the bone marrow of a mouse transplanted with CLL-HSCs of patient 7 and retransplanted into the second recipient. B cell clones in the second recipient were independent of that in the first recipients with different VDJ gene recombination, indicating that CLL-HSCs are capable of self-renewal. See also **Table S3**.

possessed mutated IGHVs, regardless of the SHM status of the original CLL cells.

B Cell Clones Are Derived from CLL-HSCs Capable of Self-renewal

To confirm that CLL-HSCs that generate clonal B cells in mice are capable of self-renewal, we performed a serial transplantation assay in patients 7 and 16 (**Table S3**). Experiments of patient 7 are shown in **Figure 4**B. The primary recipient (mouse 7-3 in **Table 1** and **Tables S2 and S3**) developed two $CD5^+$ B cell clones. We then purified $CD34^+CD38^-$ HSCs from the bone marrow of the primary recipient and retransplanted into the secondary recipient. The secondary recipient again developed two $CD5^+$ B cell clones, indicating that CLL-HSCs are capable of self-renewal. The VDJ recombination analysis showed that all four B cell clones were independent and had their own VDJ combination different from the original CLL clone. The serial transfer experiment was performed also in patient 16, and the secondary recipient gave rise to two clones independent of the one developed in the primary recipient (**Table S3**). These data collectively suggest that self-renewing CLL-HSCs but not normal HSCs are able to develop monoclonal or oligoclonal B cells as a result of in vivo selection, and that the pathogenesis of CLL could be traced up to the self-renewing HSC stage.

CLL-HSCs Do Not Have Chromosomal Abnormalities Related to CLL Pathogenesis

CLLs frequently have aberrations in a few chromosomal regions, including del13q14, del11q23, trisomy 12, and del17p (**Döhner et al., 2000**), and some of these appear to be directly involved in pathogenesis of CLL (**Cimmino et al., 2005; Klein et al., 2010; Ouillette et al., 2008**). Therefore, we tested whether CLL-HSCs have such abnormal karyotypes. Results are shown in **Table 2**. Purified $CD19^+$ CLL cells in patients 2 and 11 possessed del13q14, and patients 1 and 3 had both del13q14 and del11q23 by FISH analysis. However, purified $CD34^+CD38^-$ CLL-HSCs and $CD33^+$ myeloid cells did not have such abnormalities in any patients, suggesting that these chromosomal abnormalities are acquired at the mature B cell stage.

To exclude the possibility that the very minor population having such abnormal karyotypes within the $CD34^+CD38^-$ CLL-HSC fraction gave rise to CLL cells, we evaluated the karyotype of B cell clones developed from purified CLL-HSCs. Purified CLL-HSCs in patients 1–3 and 11 were transplanted into

Table 2. FISH Analyses of Purified CLL Fractions and Secondary B Cell Clones

	Patients' CLL Bone Marrow					CLL-HSC-Derived B Cell Clones		
	VDJ Gene		Abnormal Karyotypes (%)			VDJ Genes		Abnormal Karyotype (%)
Patient No.	of CLL Clone	FISH Target	B Cell	Myeloid	HSC	of B Cell Clone	FISH Target	hCD45+ Cell
1	V3-66/D3-22/J4	del13q14	77.7	<2.0	<2.0	V1-2/D3-10/J6	del13q14	<2.0
		del11q23	77.0	<2.0	<2.0		del11q23	<2.0
2	V2-5/D6-19/J4	del13q14	59.9	<2.0	<2.0	V4-59/D3-16/J4	del13q14	<2.0
3	V3-23/D5-12/J4	del13q14	95.2	<2.0	<2.0	V3-48/D6-13/J6	del13q14	<2.0
		del11q23	12.5	<2.0	<2.0		del11q23	<2.0
11	V3-20/D1-26/J6	del13q14	92.6	<2.0	<2.0	V5-51/D3-9/J5	del13q14	<2.0

immunodeficient mice. In all cases, recipients again developed clonal B cell populations with VDJ recombination independent of original CLL cells, but such B cell clones have normal karyotypes: they were free from any abnormal karyotypes that original CLL cells had (**Table 2**). Thus, oncogenic events resulting from these chromosomal abnormalities are not required for CLL-HSCs to generate clonal B cells, suggesting that these abnormalities are acquired at the mature B cell stage as an additional leukemogenic event to transform into clinical CLL.

Single CLL-HSCs Prime Lymphoid Lineage-Related Genes

The fact that the CLL-HSC always generates monoclonal or oligoclonal B cell populations strongly suggests that the CLL-HSC possesses cell-intrinsic abnormalities to exhibit this phenotype. We and others have shown that priming of lineage-associated genes reflects the developmental potential of hematopoietic stem and progenitor cells (**Akashi et al., 2003; Hu et al., 1997; Miyamoto et al., 2002**). Therefore, we analyzed the expression profile of lineage-related transcription factors in $CD34^+CD38^-$ CLL-HSCs. Conventional quantitative PCR of mRNA purified from 1000 cells showed that CLL-HSCs expressed IKZF1 (IKAROS), an early lymphoid transcription factor (**Georgopoulos et al., 1992**), and early B lymphoid ones including TCF3 (E2A) and IRF8 at significantly higher levels, as compared to normal $CD34^+CD38^-$ HSCs (**Figure S3**). Other relatively late B lymphoid-related genes including EBF, PAX5, IGLL1, DNTT, and VPREB3 were not detected in either CLL-HSCs or normal HSCs (data not shown). In contrast the expression levels of myeloid-related RUNX-1 and CEBPA, myeloid/B lymphoid-related PU.1, and T lymphoid-related NOTCH1 were not different between CLL-HSCs and normal HSCs (**Figure S3**). Thus, transcription factors required at a very early stage of B cell development appeared to be primed in the CLL-HSC.

To directly assess the frequency of lymphoid-primed CLL-HSCs within the $CD34^+CD38^-$ fraction of patients with CLL, we performed the single-cell gene expression assay of CLL-HSCs, as well as of HSCs, common lymphoid progenitors (CLPs) (**Galy et al., 1995**), and proB cells from normal controls. **Figure 5**A shows the representative PCR data of CLL-HSCs from two patients and of normal HSCs from a control. The summary of data of six patients with CLL and normal controls is shown in **Figure 5**B. The data showed that only ~15% of normal HSCs expressed IKAROS, whereas ~60% of single CLL-HSCs expressed IKAROS at a detectable level in this assay system. The frequency of IKAROS-expressing cells gradually increased as normal HSCs differentiated into CLPs and then into proB cells. Similarly, cells expressing E2A and IRF8 began to appear at the CLL-HSC stage, but frequencies of cells expressing these molecules increased in CLP and proB cells. Cells expressing TDT, VPREB3, and PAX5 appeared on and after the CLP stage. In contrast, IKAROS expressing single CLL-HSCs frequently coexpressed early myeloid transcription factors such as GATA-2 and CEBPA that were progressively shut off in CLP or proB cells, reflecting their multipotency (**Figures 5**A and 5B). These data suggest that a considerable fraction of CLL-HSCs has activated early lymphoid transcription factors, presumably reflecting their cell-intrinsic priming into the lymphoid lineage.

DISCUSSION

In the present study, we showed evidence that self-renewing HSCs are involved in pathogenesis of CLL, a mature B cell neoplasm. In the xenogeneic transplantation system, both CLL-HSCs and normal HSCs showed multilineage differentiation, but only the former gave rise to clonal B cells. Such B cell clones frequently expressed CD5 and CD23 surface antigens, which are the typical phenotypic characteristics of de novo CLL. These CLL-HSC-derived B cells were monoclonal or oligoclonal but were independent of the original patients' CLL clones confirmed by VDJ recombination analyses. In contrast, normal HSCs always produced polyclonal B cells. Furthermore, patients with CLL had ~5-fold higher numbers of polyclonal proB cells as compared to normal individuals, and CLL-HSCs frequently displayed the primed expression of early lymphoid transcription factors including IKAROS and E2A at the single-cell level. After transplantation into xenogeneic recipients, CLL-HSCs produced higher numbers of polyclonal proB cells than normal HSCs. CLL-HSCs did not have abnormal karyotypes frequently detected in CLL (**Table 2**). These data suggest that the CLL-HSC possesses cell-intrinsic abnormalities for enhanced production of polyclonal B cell progenitors, and among whose progeny, B cell clones with CLL or MBL phenotype selectively expand in vivo.

In human the $CD34^+CD38^-$ population in the bone marrow contained most, if not all, of HSCs (**Bhatia et al., 1997; Terstappen et al., 1991**). In HSC subpopulation analysis (**Figures 1**A and 1B), more than 90% of the $CD34^+CD38^-$ cells consisted of $CD90^+CD45RA^-$ LT-HSCs (~60%) and $CD90^-CD45RA^-$ multipotential progenitors (~30%) (**Majeti et al., 2007**), and the

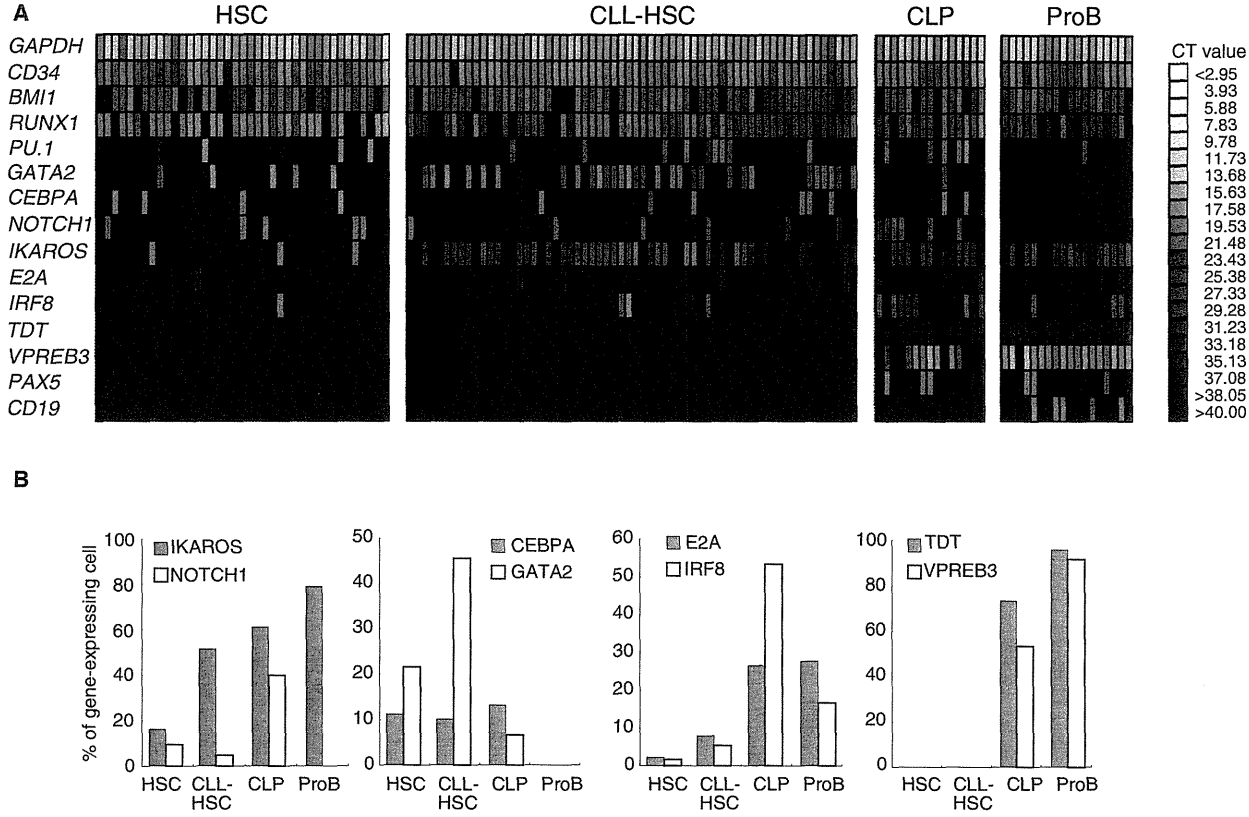

Figure 5. Lymphoid-Lineage Gene Priming in Single CLL-HSCs

(A) Single-cell quantitative gene expression analyses of CLL-HSCs, and of normal HSCs, CLP, and proB cells. Each lane represents the analysis of single cells. IKAROS, E2A, and IRF8 were more frequently expressed in CLL-HSCs as compared to normal HSCs. IKAROS was expressed in >50% of single CLL HSCs, but only in 15% of single normal HSCs, suggesting that CLL-HSCs are primed to the lymphoid lineage. In contrast, other myeloid or T-lymphoid transcription factors including CEBPA, RUNX1, PU.1, and NOTCH1 did not differ between normal HSCs and CLL-HSCs. Representative results are shown. Conventional quantitative PCR analyses of lineage-related genes in CLL-HSCs and normal HSCs are shown in **Figure S3**.

(B) The summary of frequencies of cells expressing the listed genes in stem and progenitor cell fractions (control n = 6, CLL n = 6).

$CD90^{-}CD45RA^{+}$ population that was reported to initiate lymphomyeloid differentiation (**Doulatov et al., 2010; Goardon et al., 2011**) constituted only a minor (<10%) population in both normal and CLL bone marrow. Furthermore, quantitative digital PCR analysis showed that the expression pattern of major transcription factors in single cells in the $CD34^{+}CD38^{-}$ HSC or CLL-HSC fractions appeared to be homogeneous, and among >200 single cells analyzed, none of them expressed relatively late lymphoid molecules such as TDT, VPREB3, and PAX5 that were expressed in the majority of CLP and proB cells (**Figure 5**). Thus, the vast majority of the $CD34^{+}CD38^{-}$ population is uncommitted stem or progenitor cells. However, it was still possible that the purified $CD34^{+}CD38^{-}$ CLL-HSC population contained a few original CLL clones with recombined VDJ genes, from which the B cell clones were expanded to become visible after transplantation. This possibility was excluded based on results of the following experiments. First, CLL-HSCs as well as CLL-like B cell clones developed in xenogeneic recipients did not have karyotypic anomaly such as del13q14 and del11q23 that the original CLL cells had. Second, the CLL-HSC purified from a single patient always produced independent B cell clones in multiple recipients (**Figure 4**A). Third, purified CLL-HSCs were capable of self-renewal as shown in the serial transplantation experiment (**Figure 4**B), and the secondary recipient developed B cell clones independent of those in the primary recipient (**Table S3**). Collectively, the CLL-HSC fraction is the self-renewing population not contaminated with B cell clones. Our hypothesis on development of CLL is schematized in **Figure 6**.

It has been shown that virtually all patients with CLL have a precursor state such as MBL before it develops into clinically evident CLL (**Landgren et al., 2009**). Around 20%–70% of patients with MBL have more than one B cell clone (**Dagklis et al., 2009; Lanasa et al., 2010; Nieto et al., 2009**), whereas only ~10% of patients with CLL have two or more CLL clones (**Sanchez et al., 2003**). Progression into CLL is seen in a fraction of patients with MBL. A previous cohort study reported that during this process, one of the MBL clones was selected to develop into CLL (**Landgren et al., 2009**). B cell clones that arose from CLL-HSCs in our system appeared to resemble MBL, rather than CLL: more than one B cell clone was present in 13 out of 25

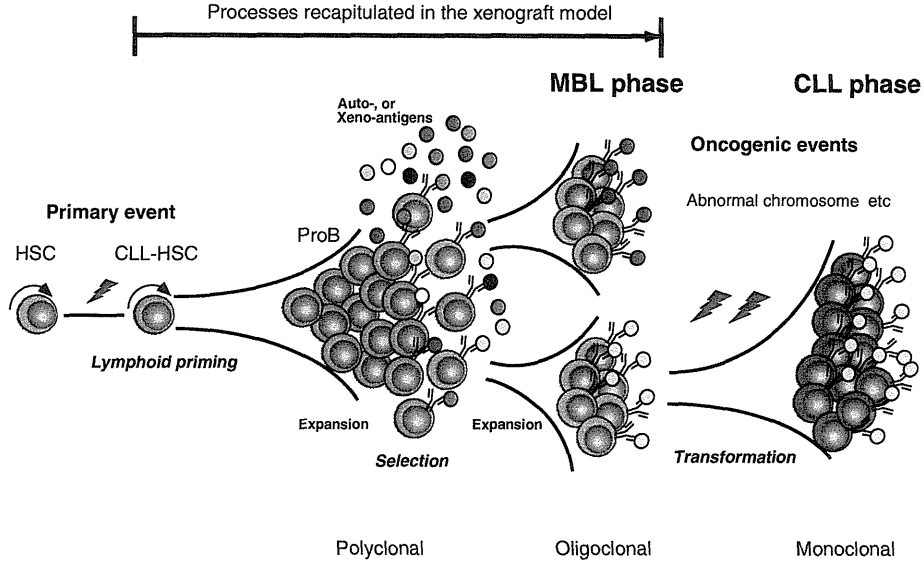

Figure 6. Schematic Presentation of Human CLL Development Based on the Xenogeneic Transplantation Model
CLL-HSCs have accumulated genetic abnormalities that might play a role in amplified B cell differentiation, and produce a high number of polyclonal B cells carrying the same genetic aberrations. B cell clones are selected, and expanded in response to BCR signaling driven presumably by xeno-antigens, simulating progression of MBL. Additional abnormalities such as aberrant karyotypes might play a role in progression from MBL into human CLL. This final step was not recapitulated in the xenograft model.

(~50%) mice analyzed in our experiments (**Table 1**). Importantly, such B cell clones developed as short as 3 months after xenogeneic transplantation, and they did not have chromosomal abnormalities that original patients had. Somatic mutation status of B cell clones also implies their MBL-like characteristics. It has been shown that ~90% of MBL clones carry IGHV genes with somatic mutation, whereas ~60% of CLL clones have mutated IGHV genes. In the present study 13 out of 16 patients with CLL had CLL cells with mutated IGHVs, whereas after transplantation, 45 out of 50 B cell clones developed from CLL-HSCs had mutated IGHVs. The frequent usage of mutated IGHV in B cell clones again suggests that these B cell clones developed in mice might correspond to de novo MBL. Collectively, xenogeneic transplantation of CLL-HSCs in immunodeficient mice could recapitulate at least the progression into the MBL, suggesting that the primary genetic abnormality to cause MBL might be acquired already at the long-term self-renewing CLL-HSC level.

It is still unknown as to how such MBL clones are expanded, and are selected in vivo to become CLL. Interestingly, MBL clones that progress into CLL use a biased set of VH genes including VH1, 3, and 4, which de novo CLL cells preferentially use (**Landgren et al., 2009; Rawstron et al., 2008**). It is also known that CLL cells express a restricted BCR repertoire, including antibodies with quasi-identical CDR3 (**Ghiotto et al., 2004; Messmer et al., 2004; Tobin et al., 2003, 2004; Widhopf et al., 2004**). The striking degree of structural restriction of the entire BCR in CLL suggests that common or similar antigens are recognized by CLL cells, and supports the hypothesis that an antigen-driven process contributes to CLL pathogenesis (**Zenz et al., 2010**). Such antigens may include autoantigens, partly because CLL clones frequently produce autoreactive antibodies (**Borche et al., 1990; Bröker et al., 1988; Sthoeger et al., 1989**). In this context it is possible that human CLL cells could not engraft into mice because the BCR of patients' CLL cells cannot recognize xeno-antigens in mice.

Similarly, in our xenogeneic transplantation analysis, CLL-HSC-derived B cell clones but not normal HSC-derived polyclonal B cells preferentially used the VH1, VH3, and VH4 (**Table S2**), indicating that propensity of biased usage of VH genes is preserved in CLL-HSCs, but not normal HSCs. The possible explanation for this phenomenon is that B cell clones with these VH genes were preferentially selected by BCR signals triggered by antigens, or that CLL-HSCs possess some cell-intrinsic defects in recombining other than these VH genes. Interestingly, CDR analysis of CLL-HSC-derived B cell clones showed that >65% of CDR3 amino acids between clonal B cells in mice 10-3 and 12 were identical, and three independent B cell clones in mice 3, 7-3, and 12 shared >60% of CDR3 amino acids (**Figure S2** and **Table S2**). These independent B cell clones correspond to the moderate level of CDR3 homology defined by a previous study (**Tobin et al., 2004**), suggesting that the BCR of these B cell clones may recognize common xeno-antigen to expand, and antigen-driven process may play a critical role in clonal B cell development even in our xenogeneic transplantation model.

Previous data have shown that chromosomal abnormalities often found in patients with CLL, such as del13q14 and del11q23, are directly linked to the leukemogenesis of CLL. For example deletion of 13q14 causes loss of miR15a and miR16-1 that target Bcl-2, resulting in the upregulation of Bcl-2 (**Cimmino et al., 2005**) and proliferation of CLL cells (**Klein**

et al., 2010). Our data clearly show that expansion of B cell clones does not require such signaling caused by chromosomal aberration (Table 2). Thus, the acquisition of abnormal karyotypes is not necessary for MBL-like clonal B cell development but might play a role in progression from MBL into clinical CLL (Figure 6).

Thus, the propensity to progress into CLL is acquired already at the HSC level. HSCs in patients with CLL are able to produce a high number of B cells. Such B cells should carry the genetic abnormality identical to HSCs, which might play a role in clonal expansion after they differentiate into B cells presumably collaborating with BCR signaling in response to auto-antigens. Further accumulation of genetic alteration(s) such as chromosomal abnormalities might cause transformation of a fraction of MBL clones into clinical CLL. Accordingly, our results suggest that the blockage of BCR signaling, by Syk inhibitors (Friedberg et al., 2010; Suljagic et al., 2010), for example, might be useful to inhibit development of human MBL, or its progression into CLL. Our xenogeneic transplantation experiments may not recapitulate the full picture of CLL progression, but they do recapitulate the development of MBL starting from human HSCs of patients with CLL (Figure 6). Our data suggest that even in human CLL, the primary leukemogenic event involves multipotent, self-renewing HSCs. Identification of the intrinsic abnormality of HSCs in patients with CLL should be the key to finding the ultimate therapeutic target in human CLL.

EXPERIMENTAL PROCEDURES

Clinical Samples

Diagnostic and follow-up bone marrow or blood samples of 16 patients with CLL were used in this study. All cases were immunophenotyped as previously described (Chiorazzi et al., 2005) and met the diagnostic criteria of the National Cancer Institute Working Group (NCI-WG) (Hallek et al., 2008). Table S1 lists the patient characteristics. Human age-matched adult bone marrow and peripheral blood cells were obtained from healthy donors or purchased from AllCells Inc. (Emeryville, CA, USA). Informed consent was obtained from all patients and controls in accordance with the Helsinki Declaration of 1975 that was revised in 1983. The Institutional Review Board of Kyushu University Hospital approved all research on human subjects.

Antibodies, Cell Staining, and Sorting

Human HSCs, progenitors, and other hematopoietic cells were stained and sorted by FACS Aria (BD Biosciences, San Jose, CA, USA). The bone marrow mononuclear cells (MNCs) were concentrated by standard gradient centrifugation, and the $CD34^+$ cells were enriched from MNCs by using the Indirect CD34 MicroBead Kit (Miltenyi Biotec, Bergisch-Gladbach, Germany). The HSC population used for xenotransplant or PCR analyses purified as $CD34^+CD38^-$ cells from the fraction does not express lineage antigens as described below. In some cases $CD34^+CD38^-CD90^+$ cells were used for the xenotransplantation assay (Table 1). Briefly, for the FACS analysis or sorting of human bone marrow cell fractions, cells were stained with a Cy5-PE- or PC5-conjugated lineage cocktail, including anti-CD3 (HIT3a), CD4 (RPA-T4), CD8 (RPA-T8), CD10 (HI10a), CD19 (HIB19), CD20 (2H7), CD11b (ICFR44), CD14 (RMO52), CD56 (NKH-1), and GPA (GA-R2). Cy5-PE-conjugated CD10, CD19, and CD20 monoclonal antibodies were excluded from lineage cocktail in the B-lymphoid progenitor assay. Cells were further stained with FITC-conjugated anti-CD10 (SS2/36), anti-CD34 (8G12) or anti-CD90 (5E10), PE-conjugated, anti-CD19 (HIB19), APC-conjugated anti-CD34 (8G12) or anti-CD38 (HIT2), PE-Cy7-conjugated anti-CD5 (L17F12), anti-CD19 (SJ25C1), anti-CD34 (8G12) or anti-CD38 (HIT2), Pacific Blue-conjugated anti-CD45RA (HI100), and biotinylated anti-CD38 (HIT2). For analysis of human cells developed in the immunodeficient mice, FITC-conjugated anti-CD5 (UCTH2), anti-CD33 (HIM3-4) or anti-human IgM (G20-127), PE-conjugated anti-CD5 (UCHT2), anti-CD20 (L27), anti-CD23 (EBVCS-5), or anti-CD45 (HI30), APC-conjugated anti-CD45 (J.33) monoclonal antibodies were used. Streptavidin-conjugated APC-Cy7 or PE-Cy7 was used to visualize biotinylated antibodies (BD PharMingen, San Jose, CA, USA). Nonviable cells were excluded by propidium iodide (PI) staining. Appropriate isotype-matched, irrelevant control monoclonal antibodies were used to determine the level of background staining. The sorted cells were subjected to an additional round of sorting using the same gate to eliminate contaminating cells and doublets. For single-cell assays an automatic cell-deposition unit system (BD Biosciences, San Jose, CA, USA) was used.

FISH Analysis

FISH analysis was performed on interphase nuclei from the bone marrow or blood cells. The probe sets detect 13q- (D13S319 at 13q14 and LAMP1 at 13q34), 12 (D12Z3 at CEN12), and 11q- (ATM at 11q23 and D11Z1 at CEN11). The specimens in this study were analyzed in a random order, by blinded observers. Intact, nonoverlapping nuclei were scored. A total of 1000 nuclei were analyzed for each probe set for each patient.

Xenogeneic Transplantation

NRG mice (stock #7799) (Pearson et al., 2008) (purchased from The Jackson Laboratory) and NOD.Cg-Prkdc^{scid}IL-2rg^{tm1Wjl}/Sz (NSG) mice (Shultz et al., 2005; Ishikawa et al., 2005) were used for xenogeneic transplantation assays. Mice were housed in a specific pathogen-free facility in micro-isolator cages at the Kyushu University (Fukuoka, Japan) or RIKEN Center for Allergy and Immunology (Kanagawa, Japan). Animal experiments were performed in accordance with institutional guidelines approved by the animal care committee of each institute. For the reconstitution assays, sorted cells were transplanted into irradiated (100 cGy) NSG newborns via a facial vein within 48 hr of birth (Ishikawa et al., 2005) or into sublethally irradiated NRG adult mice (4.8 Gy) via a tail vein as previously reported (Kikushige et al., 2010).

IGH Gene Rearrangement Analysis and Subcloning of PCR Products

Genomic DNA was extracted by Micro Kit (QIAGEN) according to the manufacturer's instructions. Multiplex PCR assays were employed to detect clonal B cell population (van Dongen et al., 2003). To evaluate the IGH gene rearrangement of a small number of sorted cells, semi-nested PCR assays were performed (d'Amore et al., 1997; Ramasamy et al., 1992; Reed et al., 1993). The clonal PCR product was excised from gel, purified by QIAquick Spin (QIAGEN), and directly sequenced with the heavy-chain primer by ABI 3730 Genetic analyzer (Applied Biosystems).

Subcloning was performed to detect clonal bands within polyclonal background, by using the TOPO TA Cloning kit (Invitrogen). The PCR products were ligated into the vector and transformed in *Escherichia coli* cells according to the manufacturer's recommendation. At least 12 colonies were selected and sequenced to confirm clonal expansion. The sequence results were analyzed on the IMGT tools (Giudicelli et al., 2004) and IgBLAST, and aligned to the closest match with the germline IGHV segment. Sequencing results with a germline identity of less than 98% were regarded as mutated, whereas those with a germline identity of 98% or more were regarded as unmutated according to previous studies (Damle et al., 1999; Hamblin et al., 1999).

Single-Cell Quantitative PCR

For single-cell quantitative PCR analysis, single $CD34^+CD38^-Lin^-$HSC, $CD34^+CD38^+CD10^+CD19^-Lin^-$CLP (Galy et al., 1995), or $CD34^+CD38^+CD10^+CD19^+Lin^-$proB cell was sorted directly into the mixture of CellsDirect 2× Reaction Mix (CellsDirect™; Invitrogen), 0.2× TaqMan Assay Mix (Applied Biosystems), and SuperScript™ III RT/Platinum Taq Mix (Invitrogen) according to the protocol of BioMark™ Dynamic Array (Fluidigm, CA, USA). After sorting single cells into 96-well plates, reverse transcription (RT) and specific target amplification (STA) were performed. Temperature setting for RT was 15 min at 50°C, and after RT reaction, samples were incubated for 2 min 95°C. Thermal-cycling settings for STA were 22 cycles of 95°C for 15 s and 60°C for 4 min. After RT and STA reaction, preamplified cDNA was diluted with TE buffer (1:5). Single-cell quantitative PCR was performed using BioMark™ 48 × 48 or 96 × 96 Dynamic Array. Data were analyzed by BioMark™ Real-Time PCR Analysis Software v2.0 (Fluidigm, CA, USA). TaqMan Gene

Expression Assay Mixes for all the genes analyzed in this study were purchased from Applied Biosystems.

Statistical Analysis

Data were presented as mean ± standard deviation. The significance of the differences between groups was determined by using Student's t test. p values <0.05 were considered statistically significant.

SUPPLEMENTAL INFORMATION

Supplemental Information includes three figures and three tables and can be found with this article online at **doi:10.1016/j.ccr.2011.06.029**.

ACKNOWLEDGMENTS

We thank Drs. Jerome Ritz and Tetsuya Fukuda for helpful discussion. This work was supported in part by a Grant-in-Aid from the Ministry of Education, Culture, Sports, Science and Technology in Japan (to K.A. and T.M.) and a Grant-in-Aid from the Ministry of Health, Labour and Welfare in Japan (to K.A.).

Received: February 28, 2011
Revised: May 27, 2011
Accepted: June 30, 2011
Published: August 15, 2011

REFERENCES

Akashi, K., He, X., Chen, J., Iwasaki, H., Niu, C., Steenhard, B., Zhang, J., Haug, J., and Li, L. (2003). Transcriptional accessibility for genes of multiple tissues and hematopoietic lineages is hierarchically controlled during early hematopoiesis. Blood *101*, 383–389.

Anderson, K., Lutz, C., van Delft, F.W., Bateman, C.M., Guo, Y., Colman, S.M., Kempski, H., Moorman, A.V., Titley, I., Swansbury, J., et al. (2011). Genetic variegation of clonal architecture and propagating cells in leukaemia. Nature *469*, 356–361.

Bhatia, M., Wang, J.C., Kapp, U., Bonnet, D., and Dick, J.E. (1997). Purification of primitive human hematopoietic cells capable of repopulating immune-deficient mice. Proc. Natl. Acad. Sci. USA *94*, 5320–5325.

Bonnet, D., and Dick, J.E. (1997). Human acute myeloid leukemia is organized as a hierarchy that originates from a primitive hematopoietic cell. Nat. Med. *3*, 730–737.

Borche, L., Lim, A., Binet, J.L., and Dighiero, G. (1990). Evidence that chronic lymphocytic leukemia B lymphocytes are frequently committed to production of natural autoantibodies. Blood *76*, 562–569.

Bröker, B.M., Klajman, A., Youinou, P., Jouquan, J., Worman, C.P., Murphy, J., Mackenzie, L., Quartey-Papafio, R., Blaschek, M., Collins, P., et al. (1988). Chronic lymphocytic leukemic (CLL) cells secrete multispecific autoantibodies. J. Autoimmun. *1*, 469–481.

Caligaris-Cappio, F., and Ghia, P. (2008). Novel insights in chronic lymphocytic leukemia: are we getting closer to understanding the pathogenesis of the disease? J. Clin. Oncol. *26*, 4497–4503.

Chiorazzi, N., and Ferrarini, M. (2003). B cell chronic lymphocytic leukemia: lessons learned from studies of the B cell antigen receptor. Annu. Rev. Immunol. *21*, 841–894.

Chiorazzi, N., Rai, K.R., and Ferrarini, M. (2005). Chronic lymphocytic leukemia. N. Engl. J. Med. *352*, 804–815.

Cimmino, A., Calin, G.A., Fabbri, M., Iorio, M.V., Ferracin, M., Shimizu, M., Wojcik, S.E., Aqeilan, R.I., Zupo, S., Dono, M., et al. (2005). miR-15 and miR-16 induce apoptosis by targeting BCL2. Proc. Natl. Acad. Sci. USA *102*, 13944–13949.

Dagklis, A., Fazi, C., Sala, C., Cantarelli, V., Scielzo, C., Massacane, R., Toniolo, D., Caligaris-Cappio, F., Stamatopoulos, K., and Ghia, P. (2009). The immunoglobulin gene repertoire of low-count chronic lymphocytic leukemia (CLL)-like monoclonal B lymphocytosis is different from CLL: diagnostic implications for clinical monitoring. Blood *114*, 26–32.

Damle, R.N., Wasil, T., Fais, F., Ghiotto, F., Valetto, A., Allen, S.L., Buchbinder, A., Budman, D., Dittmar, K., Kolitz, J., et al. (1999). Ig V gene mutation status and CD38 expression as novel prognostic indicators in chronic lymphocytic leukemia. Blood *94*, 1840–1847.

d'Amore, F., Stribley, J.A., Ohno, T., Wu, G., Wickert, R.S., Delabie, J., Hinrichs, S.H., and Chan, W.C. (1997). Molecular studies on single cells harvested by micromanipulation from archival tissue sections previously stained by immunohistochemistry or nonisotopic in situ hybridization. Lab. Invest. *76*, 219–224.

Döhner, H., Stilgenbauer, S., Benner, A., Leupolt, E., Kröber, A., Bullinger, L., Döhner, K., Bentz, M., and Lichter, P. (2000). Genomic aberrations and survival in chronic lymphocytic leukemia. N. Engl. J. Med. *343*, 1910–1916.

Doulatov, S., Notta, F., Eppert, K., Nguyen, L.T., Ohashi, P.S., and Dick, J.E. (2010). Revised map of the human progenitor hierarchy shows the origin of macrophages and dendritic cells in early lymphoid development. Nat. Immunol. *11*, 585–593.

Dürig, J., Ebeling, P., Grabellus, F., Sorg, U.R., Möllmann, M., Schütt, P., Göthert, J., Sellmann, L., Seeber, S., Flasshove, M., et al. (2007). A novel non-obese diabetic/severe combined immunodeficient xenograft model for chronic lymphocytic leukemia reflects important clinical characteristics of the disease. Cancer Res. *67*, 8653–8661.

Fais, F., Ghiotto, F., Hashimoto, S., Sellars, B., Valetto, A., Allen, S.L., Schulman, P., Vinciguerra, V.P., Rai, K., Rassenti, L.Z., et al. (1998). Chronic lymphocytic leukemia B cells express restricted sets of mutated and unmutated antigen receptors. J. Clin. Invest. *102*, 1515–1525.

Friedberg, J.W., Sharman, J., Sweetenham, J., Johnston, P.B., Vose, J.M., Lacasce, A., Schaefer-Cutillo, J., De Vos, S., Sinha, R., Leonard, J.P., et al. (2010). Inhibition of Syk with fostamatinib disodium has significant clinical activity in non-Hodgkin lymphoma and chronic lymphocytic leukemia. Blood *115*, 2578–2585.

Galy, A., Travis, M., Cen, D., and Chen, B. (1995). Human T, B, natural killer, and dendritic cells arise from a common bone marrow progenitor cell subset. Immunity *3*, 459–473.

Georgopoulos, K., Moore, D.D., and Derfler, B. (1992). Ikaros, an early lymphoid-specific transcription factor and a putative mediator for T cell commitment. Science *258*, 808–812.

Ghiotto, F., Fais, F., Valetto, A., Albesiano, E., Hashimoto, S., Dono, M., Ikematsu, H., Allen, S.L., Kolitz, J., Rai, K.R., et al. (2004). Remarkably similar antigen receptors among a subset of patients with chronic lymphocytic leukemia. J. Clin. Invest. *113*, 1008–1016.

Giudicelli, V., Chaume, D., and Lefranc, M.P. (2004). IMGT/V-QUEST, an integrated software program for immunoglobulin and T cell receptor V-J and V-D-J rearrangement analysis. Nucleic Acids Res. *32* (Web Server issue), W435–W440.

Goardon, N., Marchi, E., Atzberger, A., Quek, L., Schuh, A., Soneji, S., Woll, P., Mead, A., Alford, K.A., Rout, R., et al. (2011). Coexistence of LMPP-like and GMP-like leukemia stem cells in acute myeloid leukemia. Cancer Cell *19*, 138–152.

Hallek, M., Cheson, B.D., Catovsky, D., Caligaris-Cappio, F., Dighiero, G., Döhner, H., Hillmen, P., Keating, M.J., Montserrat, E., Rai, K.R., and Kipps, T.J.; International Workshop on Chronic Lymphocytic Leukemia. (2008). Guidelines for the diagnosis and treatment of chronic lymphocytic leukemia: a report from the International Workshop on Chronic Lymphocytic Leukemia updating the National Cancer Institute-Working Group 1996 guidelines. Blood *111*, 5446–5456.

Hamblin, T.J., Davis, Z., Gardiner, A., Oscier, D.G., and Stevenson, F.K. (1999). Unmutated Ig V(H) genes are associated with a more aggressive form of chronic lymphocytic leukemia. Blood *94*, 1848–1854.

Hervé, M., Xu, K., Ng, Y.S., Wardemann, H., Albesiano, E., Messmer, B.T., Chiorazzi, N., and Meffre, E. (2005). Unmutated and mutated chronic lymphocytic leukemias derive from self-reactive B cell precursors despite expressing different antibody reactivity. J. Clin. Invest. *115*, 1636–1643.

Hiramatsu, H., Nishikomori, R., Heike, T., Ito, M., Kobayashi, K., Katamura, K., and Nakahata, T. (2003). Complete reconstitution of human lymphocytes from

cord blood CD34+ cells using the NOD/SCID/gammacnull mice model. Blood *102*, 873–880.

Hu, M., Krause, D., Greaves, M., Sharkis, S., Dexter, M., Heyworth, C., and Enver, T. (1997). Multilineage gene expression precedes commitment in the hemopoietic system. Genes Dev. *11*, 774–785.

Hummel, J.L., Lichty, B.D., Reis, M., Dubé, I., and Kamel-Reid, S. (1996). Engraftment of human chronic lymphocytic leukemia cells in SCID mice: in vivo and in vitro studies. Leukemia *10*, 1370–1376.

Huntly, B.J., Shigematsu, H., Deguchi, K., Lee, B.H., Mizuno, S., Duclos, N., Rowan, R., Amaral, S., Curley, D., Williams, I.R., et al. (2004). MOZ-TIF2, but not BCR-ABL, confers properties of leukemic stem cells to committed murine hematopoietic progenitors. Cancer Cell *6*, 587–596.

Ishikawa, F., Yasukawa, M., Lyons, B., Yoshida, S., Miyamoto, T., Yoshimoto, G., Watanabe, T., Akashi, K., Shultz, L.D., and Harada, M. (2005). Development of functional human blood and immune systems in NOD/SCID/IL2 receptor gamma chain(null) mice. Blood *106*, 1565–1573.

Jin, L., Hope, K.J., Zhai, Q., Smadja-Joffe, F., and Dick, J.E. (2006). Targeting of CD44 eradicates human acute myeloid leukemic stem cells. Nat. Med. *12*, 1167–1174.

Jin, L., Lee, E.M., Ramshaw, H.S., Busfield, S.J., Peoppl, A.G., Wilkinson, L., Guthridge, M.A., Thomas, D., Barry, E.F., Boyd, A., et al. (2009). Monoclonal antibody-mediated targeting of CD123, IL-3 receptor alpha chain, eliminates human acute myeloid leukemic stem cells. Cell Stem Cell *5*, 31–42.

Kikushige, Y., Shima, T., Takayanagi, S., Urata, S., Miyamoto, T., Iwasaki, H., Takenaka, K., Teshima, T., Tanaka, T., Inagaki, Y., and Akashi, K. (2010). TIM-3 is a promising target to selectively kill acute myeloid leukemia stem cells. Cell Stem Cell *7*, 708–717.

Klein, U., Tu, Y., Stolovitzky, G.A., Mattioli, M., Cattoretti, G., Husson, H., Freedman, A., Inghirami, G., Cro, L., Baldini, L., et al. (2001). Gene expression profiling of B cell chronic lymphocytic leukemia reveals a homogeneous phenotype related to memory B cells. J. Exp. Med. *194*, 1625–1638.

Klein, U., Lia, M., Crespo, M., Siegel, R., Shen, Q., Mo, T., Ambesi-Impiombato, A., Califano, A., Migliazza, A., Bhagat, G., and Dalla-Favera, R. (2010). The DLEU2/miR-15a/16-1 cluster controls B cell proliferation and its deletion leads to chronic lymphocytic leukemia. Cancer Cell *17*, 28–40.

Kolar, G.R., Yokota, T., Rossi, M.I., Nath, S.K., and Capra, J.D. (2004). Human fetal, cord blood, and adult lymphocyte progenitors have similar potential for generating B cells with a diverse immunoglobulin repertoire. Blood *104*, 2981–2987.

Lanasa, M.C., Allgood, S.D., Volkheimer, A.D., Gockerman, J.P., Whitesides, J.F., Goodman, B.K., Moore, J.O., Weinberg, J.B., and Levesque, M.C. (2010). Single-cell analysis reveals oligoclonality among 'low-count' monoclonal B-cell lymphocytosis. Leukemia *24*, 133–140.

Landgren, O., Albitar, M., Ma, W., Abbasi, F., Hayes, R.B., Ghia, P., Marti, G.E., and Caporaso, N.E. (2009). B-cell clones as early markers for chronic lymphocytic leukemia. N. Engl. J. Med. *360*, 659–667.

Luckey, C.J., Bhattacharya, D., Goldrath, A.W., Weissman, I.L., Benoist, C., and Mathis, D. (2006). Memory T and memory B cells share a transcriptional program of self-renewal with long-term hematopoietic stem cells. Proc. Natl. Acad. Sci. USA *103*, 3304–3309.

Majeti, R., Park, C.Y., and Weissman, I.L. (2007). Identification of a hierarchy of multipotent hematopoietic progenitors in human cord blood. Cell Stem Cell *1*, 635–645.

Majeti, R., Chao, M.P., Alizadeh, A.A., Pang, W.W., Jaiswal, S., Gibbs, K.D., Jr., van Rooijen, N., and Weissman, I.L. (2009). CD47 is an adverse prognostic factor and therapeutic antibody target on human acute myeloid leukemia stem cells. Cell *138*, 286–299.

Manz, M.G., Miyamoto, T., Akashi, K., and Weissman, I.L. (2002). Prospective isolation of human clonogenic common myeloid progenitors. Proc. Natl. Acad. Sci. USA *99*, 11872–11877.

Marti, G.E., Rawstron, A.C., Ghia, P., Hillmen, P., Houlston, R.S., Kay, N., Schleinitz, T.A., and Caporaso, N.; International Familial CLL Consortium. (2005). Diagnostic criteria for monoclonal B-cell lymphocytosis. Br. J. Haematol. *130*, 325–332.

Matsumura, T., Kametani, Y., Ando, K., Hirano, Y., Katano, I., Ito, R., Shiina, M., Tsukamoto, H., Saito, Y., Tokuda, Y., et al. (2003). Functional CD5+ B cells develop predominantly in the spleen of NOD/SCID/gammac(null) (NOG) mice transplanted either with human umbilical cord blood, bone marrow, or mobilized peripheral blood CD34+ cells. Exp. Hematol. *31*, 789–797.

Messmer, B.T., Albesiano, E., Efremov, D.G., Ghiotto, F., Allen, S.L., Kolitz, J., Foa, R., Damle, R.N., Fais, F., Messmer, D., et al. (2004). Multiple distinct sets of stereotyped antigen receptors indicate a role for antigen in promoting chronic lymphocytic leukemia. J. Exp. Med. *200*, 519–525.

Miyamoto, T., Iwasaki, H., Reizis, B., Ye, M., Graf, T., Weissman, I.L., and Akashi, K. (2002). Myeloid or lymphoid promiscuity as a critical step in hematopoietic lineage commitment. Dev. Cell *3*, 137–147.

Nieto, W.G., Almeida, J., Romero, A., Teodosio, C., Lopez, A., Henriques, A.F., Sanchez, M.L., Jara-Acevedo, M., Rasillo, A., Gonzalez, M., et al. (2009). Increased frequency (12%) of circulating CLL-like B-cell clones in healthy individuals using a high-sensitive multicolor flow cytometry approach. Blood *114*, 33–37.

Notta, F., Mullighan, C.G., Wang, J.C., Poeppl, A., Doulatov, S., Phillips, L.A., Ma, J., Minden, M.D., Downing, J.R., and Dick, J.E. (2011). Evolution of human BCR-ABL1 lymphoblastic leukaemia-initiating cells. Nature *469*, 362–367.

Ouillette, P., Erba, H., Kujawski, L., Kaminski, M., Shedden, K., and Malek, S.N. (2008). Integrated genomic profiling of chronic lymphocytic leukemia identifies subtypes of deletion 13q14. Cancer Res. *68*, 1012–1021.

Pearson, T., Shultz, L.D., Miller, D., King, M., Laning, J., Fodor, W., Cuthbert, A., Burzenski, L., Gott, B., Lyons, B., et al. (2008). Non-obese diabetic-recombination activating gene-1 (NOD-Rag1 null) interleukin (IL)-2 receptor common gamma chain (IL2r gamma null) null mice: a radioresistant model for human lymphohaematopoietic engraftment. Clin. Exp. Immunol. *154*, 270–284.

Pleyer, L., Egle, A., Hartmann, T.N., and Greil, R. (2009). Molecular and cellular mechanisms of CLL: novel therapeutic approaches. Nat. Rev. Clin. Oncol. *6*, 405–418.

Ramasamy, I., Brisco, M., and Morley, A. (1992). Improved PCR method for detecting monoclonal immunoglobulin heavy chain rearrangement in B cell neoplasms. J. Clin. Pathol. *45*, 770–775.

Rawstron, A.C., Bennett, F.L., O'Connor, S.J., Kwok, M., Fenton, J.A., Plummer, M., de Tute, R., Owen, R.G., Richards, S.J., Jack, A.S., and Hillmen, P. (2008). Monoclonal B-cell lymphocytosis and chronic lymphocytic leukemia. N. Engl. J. Med. *359*, 575–583.

Reed, T.J., Reid, A., Wallberg, K., O'Leary, T.J., and Frizzera, G. (1993). Determination of B-cell clonality in paraffin-embedded lymph nodes using the polymerase chain reaction. Diagn. Mol. Pathol. *2*, 42–49.

Rosenwald, A., Alizadeh, A.A., Widhopf, G., Simon, R., Davis, R.E., Yu, X., Yang, L., Pickeral, O.K., Rassenti, L.Z., Powell, J., et al. (2001). Relation of gene expression phenotype to immunoglobulin mutation genotype in B cell chronic lymphocytic leukemia. J. Exp. Med. *194*, 1639–1647.

Rossi, M.I., Medina, K.L., Garrett, K., Kolar, G., Comp, P.C., Shultz, L.D., Capra, J.D., Wilson, P., Schipul, A., and Kincade, P.W. (2001). Relatively normal human lymphopoiesis but rapid turnover of newly formed B cells in transplanted nonobese diabetic/SCID mice. J. Immunol. *167*, 3033–3042.

Rossi, D.J., Jamieson, C.H., and Weissman, I.L. (2008). Stems cells and the pathways to aging and cancer. Cell *132*, 681–696.

Saito, Y., Kitamura, H., Hijikata, A., Tomizawa-Murasawa, M., Tanaka, S., Takagi, S., Uchida, N., Suzuki, N., Sone, A., Najima, Y., et al. (2010). Identification of therapeutic targets for quiescent, chemotherapy-resistant human leukemia stem cells. Sci. Transl. Med. *2*, 17ra19.

Sanchez, M.L., Almeida, J., Gonzalez, D., Gonzalez, M., Garcia-Marcos, M.A., Balanzategui, A., Lopez-Berges, M.C., Nomdedeu, J., Vallespi, T., Barbon, M., et al. (2003). Incidence and clinicobiologic characteristics of leukemic B-cell chronic lymphoproliferative disorders with more than one B-cell clone. Blood *102*, 2994–3002.

Scarfò, L., Dagklis, A., Scielzo, C., Fazi, C., and Ghia, P. (2010). CLL-like monoclonal B-cell lymphocytosis: are we all bound to have it? Semin. Cancer Biol. *20*, 384–390.

Shultz, L.D., Lyons, B.L., Burzenski, L.M., Gott, B., Chen, X., Chaleff, S., Kotb, M., Gillies, S.D., King, M., Mangada, J., et al. (2005). Human lymphoid and myeloid cell development in NOD/LtSz-scid IL2R gamma null mice engrafted with mobilized human hemopoietic stem cells. J. Immunol. *174*, 6477–6489.

So, C.W., Karsunky, H., Passegué, E., Cozzio, A., Weissman, I.L., and Cleary, M.L. (2003). MLL-GAS7 transforms multipotent hematopoietic progenitors and induces mixed lineage leukemias in mice. Cancer Cell *3*, 161–171.

Stevenson, F.K., and Caligaris-Cappio, F. (2004). Chronic lymphocytic leukemia: revelations from the B-cell receptor. Blood *103*, 4389–4395.

Sthoeger, Z.M., Wakai, M., Tse, D.B., Vinciguerra, V.P., Allen, S.L., Budman, D.R., Lichtman, S.M., Schulman, P., Weiselberg, L.R., and Chiorazzi, N. (1989). Production of autoantibodies by CD5-expressing B lymphocytes from patients with chronic lymphocytic leukemia. J. Exp. Med. *169*, 255–268.

Suljagic, M., Longo, P.G., Bennardo, S., Perlas, E., Leone, G., Laurenti, L., and Efremov, D.G. (2010). The Syk inhibitor fostamatinib disodium (R788) inhibits tumor growth in the Eμ- TCL1 transgenic mouse model of CLL by blocking antigen-dependent B-cell receptor signaling. Blood *116*, 4894–4905.

Terstappen, L.W., Huang, S., Safford, M., Lansdorp, P.M., and Loken, M.R. (1991). Sequential generations of hematopoietic colonies derived from single nonlineage-committed CD34+CD38- progenitor cells. Blood *77*, 1218–1227.

Tobin, G., Thunberg, U., Johnson, A., Eriksson, I., Söderberg, O., Karlsson, K., Merup, M., Juliusson, G., Vilpo, J., Enblad, G., et al. (2003). Chronic lymphocytic leukemias utilizing the VH3-21 gene display highly restricted Vlambda2-14 gene use and homologous CDR3s: implicating recognition of a common antigen epitope. Blood *101*, 4952–4957.

Tobin, G., Thunberg, U., Karlsson, K., Murray, F., Laurell, A., Willander, K., Enblad, G., Merup, M., Vilpo, J., Juliusson, G., et al. (2004). Subsets with restricted immunoglobulin gene rearrangement features indicate a role for antigen selection in the development of chronic lymphocytic leukemia. Blood *104*, 2879–2885.

van Dongen, J.J., Langerak, A.W., Brüggemann, M., Evans, P.A., Hummel, M., Lavender, F.L., Delabesse, E., Davi, F., Schuuring, E., García-Sanz, R., et al. (2003). Design and standardization of PCR primers and protocols for detection of clonal immunoglobulin and T-cell receptor gene recombinations in suspect lymphoproliferations: report of the BIOMED-2 Concerted Action BMH4-CT98-3936. Leukemia *17*, 2257–2317.

Widhopf, G.F., 2nd, Rassenti, L.Z., Toy, T.L., Gribben, J.G., Wierda, W.G., and Kipps, T.J. (2004). Chronic lymphocytic leukemia B cells of more than 1% of patients express virtually identical immunoglobulins. Blood *104*, 2499–2504.

Zenz, T., Mertens, D., Küppers, R., Döhner, H., and Stilgenbauer, S. (2010). From pathogenesis to treatment of chronic lymphocytic leukaemia. Nat. Rev. Cancer *10*, 37–50.

European Journal of Radiology 79 (2011) e74–e79

Contents lists available at ScienceDirect

European Journal of Radiology

journal homepage: www.elsevier.com/locate/ejrad

Correlation between pretreatment or follow-up CT findings and therapeutic effect of autologous peripheral blood stem cell transplantation for interstitial pneumonia associated with systemic sclerosis

Hidetake Yabuuchi[a,*], Yoshio Matsuo[a], Hiroshi Tsukamoto[b], Shunya Sunami[a], Takeshi Kamitani[a], Shuji Sakai[c], Masamitsu Hatakenaka[a], Koji Nagafuji[b], Takahiko Horiuchi[b], Mine Harada[b], Koichi Akashi[b], Hiroshi Honda[a]

[a] Department of Clinical Radiology, Graduate School of Medical Sciences, Kyushu University, 3-1-1 Maidashi, Higashi-ku, Fukuoka 812-8582, Japan
[b] Department of Medicine and Biosystemic Science, Graduate School of Medical Sciences, Kyushu University, 3-1-1 Maidashi, Higashi-ku, Fukuoka 812-8582, Japan
[c] Department of Health Sciences, Graduate School of Medical Sciences, Kyushu University, 3-1-1 Maidashi, Higashi-ku, Fukuoka 812-8582, Japan

ARTICLE INFO

Article history:
Received 15 July 2010
Received in revised form 22 March 2011
Accepted 25 March 2011

Keywords:
Autologous peripheral blood stem cell transplantation
Interstitial pneumonia
Systemic sclerosis
High resolution CT

ABSTRACT

Purpose: To evaluate what is useful among various parameters including CT findings, laboratory parameters (%VC, %DLco, KL-6), patients related data (age, sex, duration of disease) to discriminate between responder and non-responder in patients who received autologous peripheral blood stem cell transplantation (auto-PBSCT) for interstitial pneumonia (IP) with systemic sclerosis (SSc).
Method: Auto-PBSCT and follow-up of at least one year by chest CT, serum KL-6, %VC, and %DLco were performed in 15 patients for IP with SSc. Analyzed CT findings included extent of ground-glass opacity (GGO), intralobular reticular opacity, number of segments that showed traction bronchiectasis, and presence of honeycombing. We regarded the therapeutic response of patients as responders when TLC or VC increase over 10% or DLco increase more than 15%, otherwise we have classified as non-responder. We applied univariate and multivariate analyses to find the significant indicators to discriminate responders from non-responders. $P < 0.05$ was considered statistically significant.
Results: Univariate and multivariate analyses showed that the significant parameter to discriminate responders from non-responders were pretreatment KL-6, presence of honeycombing, extent of GGO, and early change in extent of GGO. Among them, extent of GGO and early change in extent of GGO were the strongest discriminators between responders and non-responders ($P = 0.001$, 0.001, respectively).
Conclusion: Several CT findings and pretreatment KL-6 may be useful to discriminate between responder and non-responder in patients who received auto-PBSCT for IP with SSc.

1. Introduction

The frequency of interstitial pneumonia (IP) in collagen vascular disease (CVD) is relatively high **[1–4]**, and it is more common and more severe in systemic sclerosis (SSc) than in other types of CVD and is a significant cause of morbidity and mortality **[1]**. Interstitial lung fibrosis in SSc occurs at a frequency of approximately 70–90% of patients **[1,2]**, and interstitial change was evident on high resolution CT (HRCT) in 60–93% of SSc **[3–5]**.

Concerning the therapy for IP with SSc, immunosuppressive therapy using corticosteroid with or without cyclophosphamide is usually selected **[6]**, but two recent prospective randomized trials failed to demonstrate a clinically relevant major beneficial effect of intravenous cyclophosphamide as compared to placebo in the treatment of SSc-associated IP **[7,8]**. In addition, Benan et al. reported that immunosuppressive treatment is not effective in preventing the development of pulmonary involvement in SSc; however, it delays the manifestation of pulmonary symptoms for nearly 4 years **[2]**.

Autologous peripheral blood stem cell transplantation (auto-PBSCT) is a promising therapy not only for hematologic malignancy but also for refractory CVD **[9–12]**. It has been reported to have a therapeutic effect both on cutaneous symptoms and IP in SSc

Abbreviations: auto-PBSCT, autologous peripheral blood stem cell transplantation; IP, interstitial pneumonia; SSc, systemic sclerosis; GGO, ground-glass opacity; PM/DM, polymyositis/dermatomyositis; CVD, collagen vascular disease; HRCT, high resolution CT; NSIP, nonspecific interstitial pneumonia; DLco, diffusing capacity of the lung for carbon monoxide; VC, vital capacity; TLC, total lung capacity; KL-6, krebs von den lungen-6.

* Corresponding author. Tel.: +81 92 642 6727; fax: +81 92 642 6727.
E-mail address: **yabuuchi@shs.kyushu-u.ac.jp** (H. Yabuuchi).

0720-048X/$ – see front matter © 2011 Elsevier Ireland Ltd. All rights reserved.
doi:**10.1016/j.ejrad.2011.03.078**

[9–12]. However, this therapy involves risk, because transplant-related mortality has been reported to be 5–23% **[9–12]**. If we could predict the therapeutic effect with the help of pretreatment CT findings, it might be a significant factor in determining treatment choice. Over the past decade, many studies have been conducted on the effect of auto-PBSCT for IP associated SSc **[9–12]**. However, there has been no report analyzing the relation between pretreatment CT findings and the therapeutic effect on IP with SSc.

The proportions of histopathologic subtype of interstitial pneumonias associated with CVD vary; nonspecific interstitial pneumonia (NSIP) accounts for a large proportion, especially in SSc (75%) **[13]**. HRCT findings of NSIP such as the extent of traction bronchiectasis and reticular opacities or the presence of honeycombing correlates with increased fibrosis on CT-pathologic correlation according to Johkoh **[14]**.

According to a guideline for therapeutic response of IP by American thoracic society/European respiratory society, total lung capacity (TLC), vital capacity (VC), and diffusing capacity of the lung for carbon monoxide (DLco) measured using a pulmonary function test were used for markers to evaluate therepeutic response **[15]**. In addition, KL-6 (Krebs von den Lunge-6) is a mucin-like high molecular weight glycoprotein, which is strongly expressed on type II alveolar pneumocytes and bronchiolar epithelial cells, and is a useful marker for estimating the activity of IP **[16]**. We can speculate that a favorable effect could occur in cases with mild fibrosis, whereas a poor effect is likely in cases with severe fibrosis. However, transbronchial lung biopsy or video-assisted thoracoscopic surgery could not be performed in the cases who suffer from poor respiratory conditions regardless of the degree of fibrosis. For example, extensive alveolitis with mild fibrosis also cause severe respiratory condition. Hence, it might be useful to predict the degree of fibrosis based on HRCT finding for estimating the therapeutic effect.

Thus, the purpose of this study was to evaluate what is useful among various parameters including CT findings, laboratory parameter (%VC, %DLco, KL-6), patients related data (age, duration of disease) to discriminate between responder and non-responder in patients who received auto-PBSCT for IP with SSc.

2. Materials and methods

2.1. Patient selection

Between May 2002 and April 2008, 15 patients (11 women, 4 men; mean age and standard deviation, 52.9 years ± 7.3; age range, 34–63 years) received auto-PBSCT for refractory SSc and were followed up for at least 12 months by HRCT, serum KL-6, and pulmonary function test at our hospital. All 15 patients received HRCT of the chest within one month before PBSCT, and follow-up CT scans were obtained every 6 months after the PBSCT, and no patient was excluded for CT related reason. The protocol of this therapy and analysis of CT images were approved by our institutional review board.

2.2. Inclusion and exclusion criteria of auto-PBSCT and CT analysis

The inclusion criteria of auto-PBSCT for refractory SSc were determined by the Department of Collagen Vascular Disease at our hospital **[9]**. Patients with SSc were eligible when they had severe diffuse SSc that had rapidly developed over the previous 4 years. They also had to have at least one of the following: (a) pulmonary involvement including VC or DLco, 70% predicted or arterial oxygen pressure (PaO^2) at room temperature below 70 mm Hg and evidence of interstitial lung disease as defined by HRCT; (b) cardiac disease, namely reversible congestive heart failure or significant arrhythmia; and (c) renal involvement such as hypertension, persistent urine analysis abnormalities, microangiopathic haemolytic anaemia, and renal insufficiency. The inclusion criteria for CT analysis is that patients should receive HRCT of the chest within one month before PBSCT, and follow-up CT scans were obtained every 6 months after the PBSCT. The exclusion criteria of auto-PBSCT for refractory CVD were also determined by the Department of Collagen Vascular Disease at our hospital **[9]**. Patients were excluded from the study when they had uncontrolled arrhythmia, severe heart failure (ejection fraction ≦ 50%), severe pulmonary hypertension (mean pulmonary arterial pressure ≧ 50 mm Hg), an extremely low level of diffusing capacity of the lung (%DLCO ≦ 20%), or severely decreased renal function (Ccr ≦ 40 ml/min/m^2). For CT analysis, patients were excluded from the study when they did not receive HRCT of the chest within one month before or every 6 months after the PBSCT.

2.3. CT examination

All patients received HRCT of the chest within one month before PBSCT. Follow-up CT scans were obtained every 6 months after the PBSCT. These CT examinations were performed using various scanners (Toshiba Aquilion 64, Aquilion 4, and Siemens Volume Zoom). After the conventional whole thorax CT scan with 5 mm thickeness, the thin-section CT scans were obtained from the lung apices to the lung base at full inspiration level and supine position. The scan parameters for thin-slice helical scans on 4 multi-detector-row CT (Aquilion 4 and Volume Zoom) were detector row width, 4 × 1 mm; helical pitch, 5.5 or 6; slice thickness and interval, 2 or 1.25 mm/10 mm; rotation time, 0.5 or 0.75 s; field of view, 200–250 mm; 120 kVp; 160–200 mA. On the 64 multi-detector-row CT (Aquilion 64), the parameters were detector row width, 64 × 0.5 mm; helical pitch, 53; slice thickness and interval, 2 mm/10 mm; rotation time, 0.5 s; field of view, 200–250 mm; 120 kVp; 160–200 mA. These images were reconstructed by using a high-spatial-frequency algorithm. None of the patients received intravenous contrast medium.

2.4. CT evaluation

The CT images before and 6 months after PBSCT were retrospectively reviewed by two chest radiologists (Y.M. and H.Y. with 14 and 22 years experience, respectively) without clinical information or biopsy results; a consensus interpretation was reached in cases of disagreement. We used an image viewer (Rapideye, Toshiba Medical Systems, Tokyo, Japan) to review CT images. The lung window was set with a width of 1500 Hounsfield units and a window level of −600 Hounsfield units. In accordance with the previous studies of CT imaging of IP by Johkoh and Sumikawa **[14,17]**, the CT images were reviewed for the presence and the extent of areas of GGO, consolidation, honeycombing, intralobular reticular opacities, nodular opacities, interlobular septal thickening. These CT terms were in accordance with those of the Fleishner Society **[18]**. The extent of these findings was determined by visually estimating their extent in the upper, middle, and lower lung zones in each lung based on the percentage of the lung field that showed each abnormality in each zone (estimated to the nearest 10% of parenchymal involvement). The overall percentage of involvement was obtained by averaging the six zones. The upper zone was defined as the area above the level of the carina; the lower zone as the area below the level of the

Table 1
Patients' profiles, pretreatment HRCT findings, early change of HRCT findings at 6 months after PBSCT, and pretreatment KL-6, %VC, and %DLco.

Case no.	Age/sex	Pretreatment HRCT findings					Early change of HRCT findings at 6 months after PBSCT				Pretreatment laboratory parameter		
		Honeycombing	GGO (%)	Reticular opacities (%)	Traction bronchiectasis (segments)	CT pattern (UIP vs. NSIP)	Honeycombing	ΔGGO (%)	ΔReticular opacities (%)	Traction bronchiectasis (segments)	KL-6 (IU/ml)	%VC (%)	%DLco (%)
1	59F	–	40	20	9	NSIP	–	−10	−5	0	1285	53.4	36.2
2	55M	+	10	3	8	UIP	+	10	2	0	813	71.8	38.4
3	48F	–	50	5	0	NSIP	–	−20	0	4	3725	74	24.9
4	59M	+	10	25	12	UIP	+	0	0	0	2351	60.5	42.1
5	54F	–	5	3	10	NSIP	–	−2	2	0	955	84.2	53.8
6	53F	–	23.3	20	18	NSIP	–	−13.3	0	0	1507	73.6	26.3
7	34F	+	10	10	8	UIP	+	5	0	2	941	35.3	27.4
8	63F	–	13	5	0	NSIP	–	−3	0	0	495	90	77.4
9	61F	–	21.7	5	14	NSIP	–	−13.7	0	−6	2108	73.5	42.6
10	43F	–	10	3	11	NSIP	–	−5	2	1	1568	52.7	70.1
11	52M	–	20	10	16	NSIP	–	−10	2	0	2319	70.4	49.8
12	54F	+	10	3	18	UIP	+	5	7	0	617	64.1	27.1
13	54M	–	5	5	0	NSIP	–	−2	−2	0	323	91.7	74.1
14	55F	–	30	10	9	NSIP	–	−15	0	−1	2094	88	52.6
15	49F	–	40	25	18	NSIP	–	−15	−15	−2	3057	58.3	22.1

Table 2
Univariate analysis results.

Parameter	Responder	Non-responder	*P*-value
Age	53.9 ± 4.8	52.0 ± 9.2	0.63
Sex			
Male	1	3	0.57
Female	6	5	
Period	21.7 ± 12.0	59.8 ± 85.7	0.25
Pretreatment KL-6	2299.3 ± 850.7	1007.9 ± 659.9	<0.01*
Pretreatment %VC	70.2 ± 11.4	68.8 ± 19.6	0.87
Pretreatment %Dlco	36.4 ± 13.6	51.3 ± 20.6	0.13
Presence of honeycombing			
Yes	0	4	0.08*
No	7	4	
Extent of GGO	32.1 ± 11.4	9.1 ± 2.7	0.00154*
Extent of reticular opacities	13.6 ± 8.0	7.1 ± 7.6	0.14
Traction bronchiectasis	12.0 ± 6.5	8.4 ± 6.0	0.29
CT pattern			
UIP	0	3	0.2
NSIP	7	5	
Early change in extent of GGO	−13.9 ± 3.4	1.0 ± 5.1	<0.001*
Early change in extent of reticular opacities	−2.6 ± 5.9	1.4 ± 2.7	0.14
Early change in traction bronchiectasis	−0.71 ± 3.0	0.38 ± 0.74	0.38

* <0.10.

inferior pulmonary vein; and the middle zone as the area between the upper and lower zones. The extent of traction bronchiectasis was evaluated by counting the number of segments that showed involved by traction bronchiectasis among the 18 segments of the total lung.

2.5. Evaluation of therapeutic effect

We evaluated the activity of IP by TLC, VC, %VC, DLco and %DLco measured using a pulmonary function test. The TLC, VC, %VC, DLco and %DLco on the pulmonary function test were recorded one month before and 12 months after PBSCT. We regarded the therapeutic response of patients as improvement (responders) when TLC or VC increase over 10% or DLco increase more than 15%, otherwise we have classified as stable/progression (non-responder) according to a guideline for therapeutic response of IP by American thoracic society/European respiratory society **[15]**.

Table 3
Multivariate analysis results.

Parameter	Responder	Non-responder	*P*-value
Pretreatment serum KL-6	2299.3 ± 850.7	1007.9 ± 659.9	0.009
Presence of honeycombing			
Yes	0	4	0.029
No	7	4	
Extent of GGO	32.1 ± 11.4	9.1 ± 2.7	0.001
Change in extent of GGO	−13.9 ± 3.4	1.0 ± 5.1	0.001

2.6. Statistical analysis

2.6.1. Univariate analysis

For analysis of the difference in frequency of each CT findings, pretreatment laboratory parameters (%VC, %DLco, KL-6), patients related data (age, sex, duration of disease) between responders and non-responders, the Fisher's exact test or *t*-test was used.

2.6.2. Multivariate analysis

The level of significance used for inclusion in the model in multiple logistic regression was less than 0.10 at the univariate analysis. A multivariate stepwise logistic regression model was used to identify significant discriminators between responders

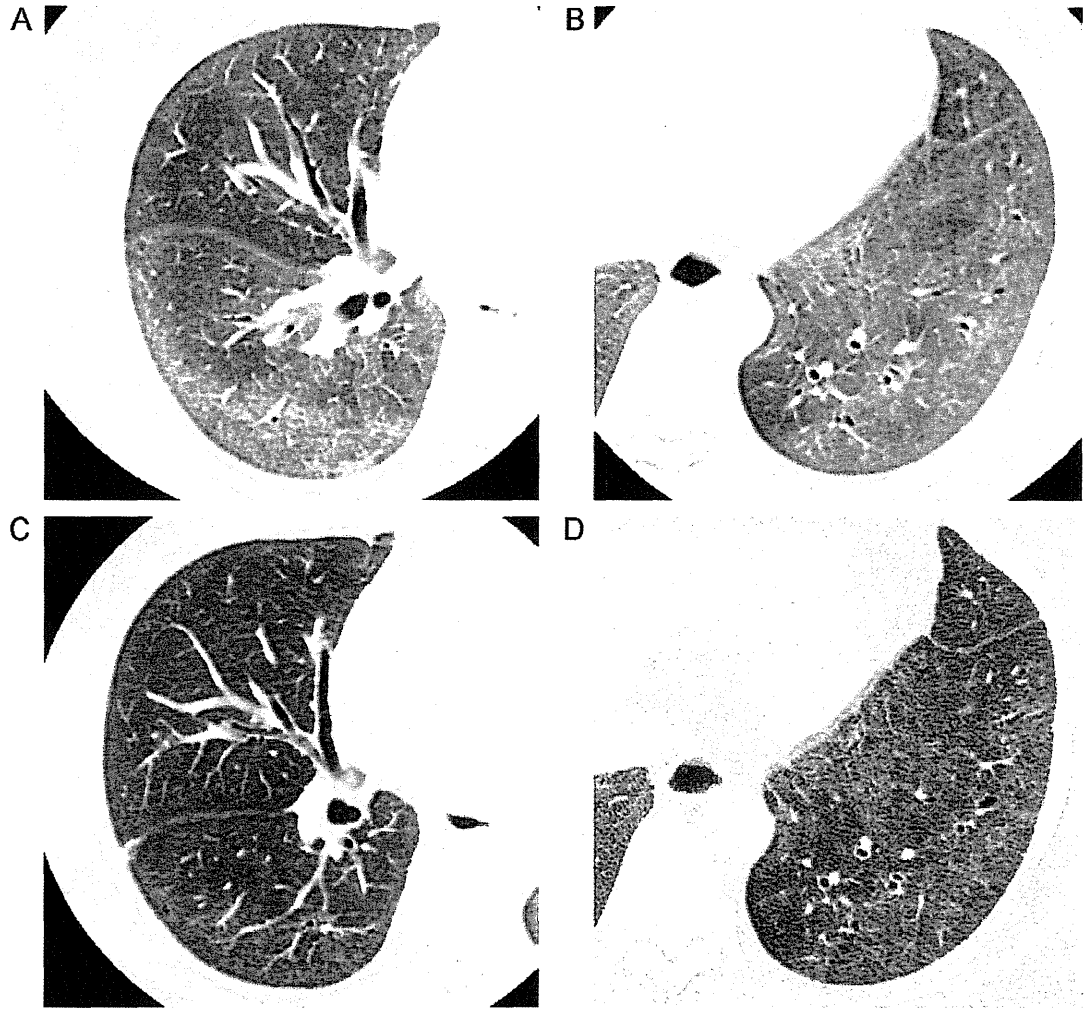

Fig. 1. HRCT in a 48-year-old woman with systemic sclerosis. (A and B) Pretreatment HRCT scan shows extended ground-glass opacities predominantly localized in the subpleural area of both lungs. Pretreatment serum KL-6 was 3725 IU/ml, and %VC was 74.0%. (C and D) HRCT scan obtained 12 months after PBSCT shows marked improvement of ground-glass opacities. Therapeutic response was considered as responding, because VC increased in 20.3% and DLco increased in 6.0%, respectively that indicated a responder.

and non-responders. *P*-values < 0.05 were considered statistically significant. Computer software (SPSS 14.0J for Windows; SPSS, Chicago, IL) was used to analyze the raw data in all statistical analyses.

3. Results

Among the CT findings that we analyzed, consolidation, nodular opacity, and interlobular septal thickening were not seen in any patients. Therefore, we could not statistically analyze these CT findings. In addition, honeycombing was seen only in 4 patients and their extent was seen only narrow part of them. In the same way, we could not analyzed the extent of honeycombing but analyzed whether honeycombing was present or not. Patients' profiles, pretreatment HRCT findings, early change of HRCT findings, pretreatment KL-6, %VC, and %DLco are given in **Table 1**.

3.1. Univariate analysis results

The significant parameters to discriminate responders from non-responders were pretreatment KL-6, presence of honeycombing, extent of GGO, and early change in extent of GGO (**Table 2**).

3.2. Multivariate analysis results

The significant parameters to discriminate responders from non-responders were pretreatment KL-6, presence of honeycombing, extent of GGO, and early change in extent of GGO. Among these parameters, extent of GGO and early change in extent of GGO were the strongest discriminators between responders and non-responders ($P = 0.001, 0.001$, respectively) (**Table 3**). **Fig. 1**A–D shows a representative case of IP with SSc that showed extensive GGO on pretreatment HRCT and a good response to PBSCT, whereas **Fig. 2**A–D shows a representative case of IP with SSc that showed honeycombing on pretreatment HRCT and a poor response to PBSCT.

4. Discussion

We have shown that the extent of GGO, pretreatment KL-6 and the presence of honeycombing on pretreatment CT and early change in the extent of GGO on follow-up CT were well correlated with the therapeutic effect of PBSCT for progressive IP associated with SSc. The presence of honeycombing on pretreatment CT could predict a poor response to PBSCT. Therefore, we should carefully consider the indications of PBSCT in patients with honeycombing

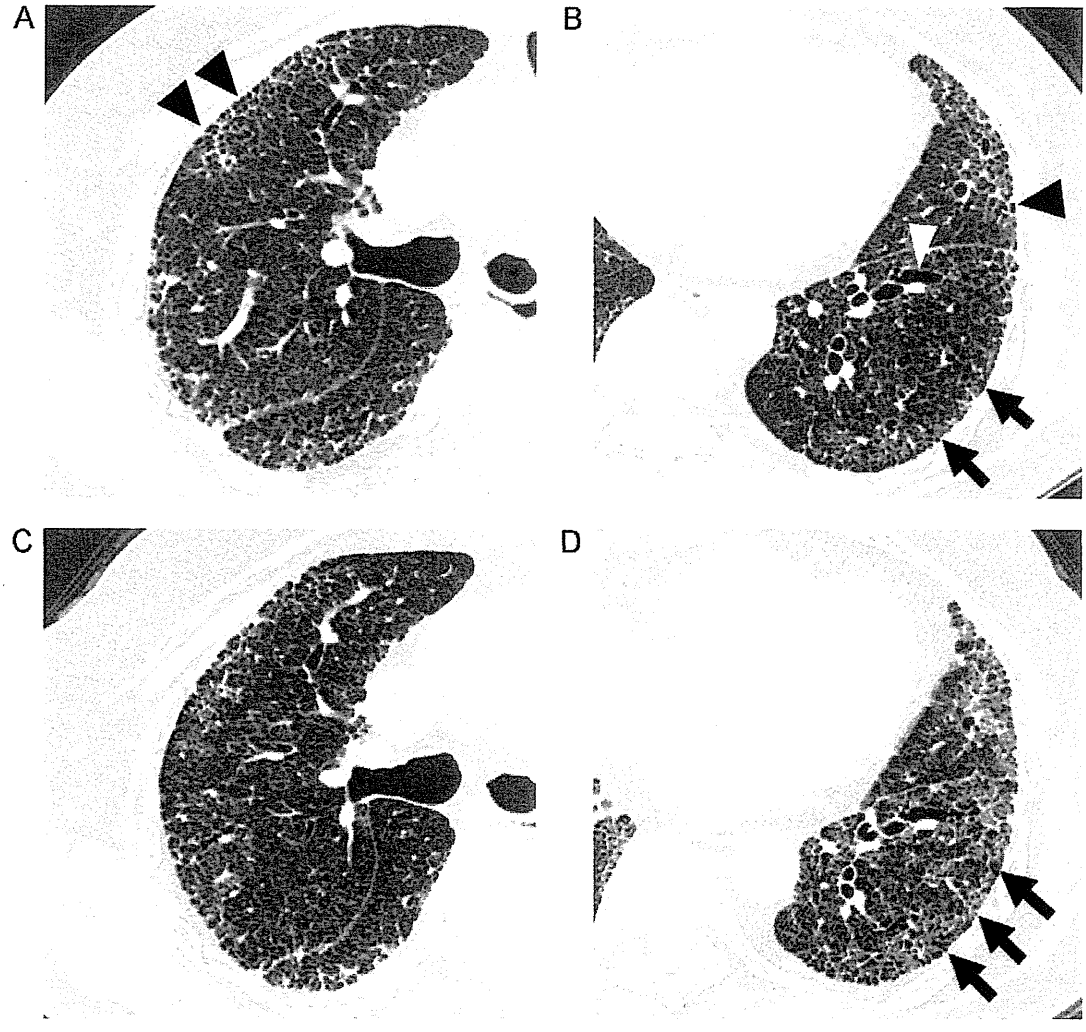

Fig. 2. HRCT in a 54-year-old woman with systemic sclerosis. (A and B) Pretreatment HRCT scan shows honeycombing (black arrow heads), reticular opacities (arrows), and traction bronchiolectasis (white arrow head) in the subpleural area of both lungs. Pretreatment serum KL-6 was 617 IU/ml, and %VC was 64.1%. (C and D) HRCT scan obtained 12 months after PBSCT shows slight deterioration of reticular opacities (arrows). Therapeutic response was considered as non-responding, because VC slightly decreased in 3.0% and DLco decreased in 2.5%, respectively that indicated a non-responder.

on pretreatment CT, because the therapeutic effect is not promising in such patients despite the risk of transplant-related mortality.

Ground-glass opacity on HRCT in patients with IP has been reported to histologically correspond to active alveolitis **[6]**, and it is believed to be a reversible change and a good prognostic factor **[19,20]**. Our results also showed that this finding correlated well with the therapeutic effect, as did previous study **[20]**. The extent of traction bronchiectasis and that of intralobular reticulation are reported to correlate with increased fibrosis in NSIP **[13]**, and these are also reported to be both reversible and irreversible changes **[21]**. These findings suggest that they may have no statistically significant correlation with the therapeutic effect in total. The presence of honeycombing on HRCT suggests that fibrosis is highly progressed in patients with IP associated with CVD. According to the correlation study between thin-section CT findings and pathologic subgroups in NSIP patients by Johkoh, honeycombing is seen almost exclusively in patients with fibrotic NSIP **[14]**. Thus, we speculate that the therapeutic effect in patients with advanced fibrosis such as honeycombing would be unfavorable.

Recent studies of histological and CT analysis of IP with SSc show a mostly NSIP pattern **[13,22]**. Bouros et al. classified the histological appearances of surgical lung biopsies performed in 80 patients with IP with SSc, and their results showed that NSIP was much more prevalent than UIP, end-stage lung disease, or other patterns **[13]**. Desai et al. compared HRCT findings of IP with SSc and those of idiopathic NSIP and IPF, and they reported that interstitial lung disease in patients with SSc is less extensive, less coarse, and characterized by a greater proportion of ground-glass opacification than that in patients with IPF **[22]**. They concluded that the CT features of lung disease in patients with SSc closely resemble those in patients with idiopathic NSIP. We speculate that PBSCT showed a good response in patients with a cellular or mild fibrotic NSIP pattern, whereas it showed a poor response in patients with a UIP or advanced fibrotic NSIP pattern based on our results.

There have been reports on the correlation with serial CT change of IP with PM/DM and pulmonary function; however, there have been no reports on the serial CT change after immunosuppressive therapy for IP with SSc. Moreover, no report has been documented concerning the pretreatment CT findings that could predict the therapeutic effect on IP with SSc. Concerning previous studies on serial HRCT changes of IP with CVD, there have been several reports that showed a good correlation between CT changes and the therapeutic effect of corticosteroids and/or other immunosuppressive drugs. Bonnefoy et al. analyzed serial CT changes of

patients with interstitial lung disease associated with PM/DM that were treated with steroids, immunosuppressive agents, or both, and reported that unfavorable evolution is constant when honeycombing is present at the initial CT **[23]**. Our results are consistent with their results in that honeycombing is an unpromising factor, although our patients were all SSc patients and were unresponsive for steroids with immunosuppressive agents and were treated with PBSCT, which is a more aggressive therapy than steroids with immunosuppressive agents.

Our study has some limitations. First, our study population was small. The limited size of our series reflects the novelty of PBSCT as a treatment for refractory CVD. Second, the observation period was only one year after the therapy, although the therapeutic effects of PBSCT on refractory CVD have been reported to present slowly within several years after initiation of the therapy **[12]**. Therefore, long-term survival or the long-term therapeutic effect on pulmonary function was unclear but warrants further investigation in future study. Constant pulmonary function or serum KL-6 data do not always mean that PBSCT has been ineffective because the absence of progression of disease activity over several years signifies the interruption of the progression of the disease. Third, histological confirmation of IP was available in only 3 of 15 patients in our study because the patients may have been too ill to undergo an invasive procedure such as video-assisted thoracoscopic surgery or transbronchial lung biopsy. Fourth, our study was conducted in a retrospective fashion, and a further cohort trial with a large population is needed to validate the true predictability of the therapeutic effect of PBSCT. However, regardless of these limitations, this is the first report to investigate the relationship between pretreatment HRCT findings and the therapeutic effect of PBSCT for IP associated with refractory SSc. We might be able to determine the indications of PBSCT based on pretreatment HRCT findings, and thus patients for whom PBSCT is expected to be ineffective can be protected from unnecessary treatment-related toxicity.

In conclusion, several CT findings including presence of honeycombing, extent of GGO, early change of the extent of GGO and pretreatment KL-6 may be useful to discriminate between responder and non-responder in patients who received auto-PBSCT for IP with SSc.

References

[1] Minai OA, Dweik RA, Arroliga AC. Manifestations of scleroderma pulmonary disease. Clin Chest Med 1998;19(4):713–31.

[2] Benan M, Hande I, Gul O. The natural course of progressive systemic sclerosis patients with interstitial lung involvement. Clin Rheumatol 2007;26(3):349–54.

[3] Remy-Jardin M, Remy J, Walaert B, et al. Pulmonary involvement in progressive systemic sclerosis: sequential evaluation with CT, pulmonary function tests, and bronchoalveolar lavage. Radiology 1993;188(2):499–506.

[4] Schurawitzki H, Stiglbauer R, Graninger W, et al. Interstitial lung disease in progressive systemic sclerosis: high-resolution CT versus radiography. Radiology 1990;176(3):755–9.

[5] Goldin JG, Lynch DA, Strollo DC, et al. High-resolution CT scan findings in patients with symptomatic scleroderma-related interstitial lung disease. Chest 2008;134(2):358–67.

[6] Okada M, Suzuki K, Matsumoto M, et al. Intermittent intravenous cyclophosphamide pulse therapy for the treatment of active interstitial lung disease associated with collagen vascular diseases. Mod Rheumatol 2007;17(2):131–6.

[7] Hoyles RK, Ellis RW, Wellsbury J, et al. A multicenter, prospective, randomized, double-blind, placebo-controlled trial of corticosteroids and intravenous cyclophosphamide followed by oral azathioprine for the treatment of pulmonary fibrosis in scleroderma. Arth Rheum 2006;54(12):3962–70.

[8] Tashkin DP, Elashoff R, Clements PJ, et al. Effects of 1-year treatment with cyclophosphamide on outcomes at 2 years in scleroderma lung disease. Am J Respir Crit Care Med 2007;176(10):1026–34.

[9] Tsukamoto H, Nagafuji K, Horiuchi T, et al. A phase I–II trial of autologous peripheral blood stem cell transplantation in the treatment of refractory autoimmune disease. Ann Rheum Dis 2006;65(4):508–14.

[10] Tyndall A, Passweg J, Gratwohl A. Haemopoietic stem cell transplantation in the treatment of severe autoimmune diseases 2000. Ann Rheum Dis 2001;60(7):702–7.

[11] Burt RK, Arnold R, Emmons R, et al. Stem cell therapy for autoimmune disease: overview of concepts from the Snowbird 2002 tolerance and tissue regeneration meeting. Bone Marrow Transplant 2003;32(8 Suppl.).

[12] Nash RA, McSweeney PA, Crofford LJ, et al. High-dose immunosuppressive therapy and autologous hematopoietic cell transplantation for severe systemic sclerosis: long-term follow-up of the US multicenter pilot study. Blood 2007;15(4):1388–96.

[13] Bouros D, Wells AU, Nicholson AG, Colby TV. Histopathologic subsets of fibrosing alveolitis in patients with systemic sclerosis and their relationship to outcome. Am J Respir Crit Care Med 2002;165(12):1581–6.

[14] Johkoh T, Muller NL, Colby TV, et al. Nonspecific interstitial pneumonia: correlation between thin-section CT findings and pathologic subgroups in 55 patients. Radiology 2002;225(1):199–204.

[15] American Thoracic Society/the European Respiratory Society. Idiopathic pulmonary fibrosis: diagnosis and treatment. International consensus statement. Am J Respir Crit Care Med 2000;161(2):646–64.

[16] Kohno N, Kyoizumi S, Awaya Y, et al. New serum indicator of interstitial pneumonitis activity. Sialylated carbohydrate antigen KL-6. Chest 1989;96(1):68–73.

[17] Sumikawa H, Johkoh T, Ichikado K, et al. Usual interstitial pneumonia and chronic idiopathic interstitial pneumonia: analysis of CT appearance in 92 patients. Radiology 2006;241(1):258–66.

[18] Austin J, Müller N, Friedman P, et al. Glossary of terms for CT of the lungs: recommendations of the nomenclature Committee of the Fleischner Society. Radiology 1996;200(2):327–31.

[19] Lynch DA, Travis WD, Müller NL, et al. Idiopathic interstitial pneumonias: CT features. Radiology 2005;236(1):10–21.

[20] Shah RM, Jimenez S, Wechsler R, et al. Significance of ground-glass opacity on HRCT in long-term follow-up of patients with systemic sclerosis. J Thorac Imaging 2007;22(2):120–4.

[21] Nishiyama O, Kondoh Y, Taniguchi H, et al. Serial high resolution CT findings innonspecific interstitial pneumonia/fibrosis. J Comput Assist Tomogr 2000;24(1):41–6.

[22] Desai SR, Veeraraghavan S, Hansell DM, et al. CT features of lung disease in patients with systemic sclerosis: comparison with idiopathic pulmonary fibrosis and nonspecific interstitial pneumonia. Radiology 2004;232(2):560–7.

[23] Bonnefoy O, Ferretti G, Calaque O, et al. Serial chest CT findings in interstitial lung disease associated with polymyositis–dermatomyositis. Eur J Radiol 2004;49(3):235.

Regenerating islet-derived 3-alpha is a biomarker of gastrointestinal graft-versus-host disease

*James L. M. Ferrara,[1] *Andrew C. Harris,[1] Joel K. Greenson,[2] Thomas M. Braun,[3] Ernst Holler,[4] Takanori Teshima,[5] John E. Levine,[1] Sung W. J. Choi,[1] Elisabeth Huber,[6] Karin Landfried,[4] Koichi Akashi,[5] Mark Vander Lugt,[1] Pavan Reddy,[7] Alice Chin,[8] Qing Zhang,[8] Samir Hanash,[8] and Sophie Paczesny[1]

Departments of [1]Pediatrics, [2]Pathology, and [3]Biostatistics, University of Michigan, Ann Arbor, MI; [4]Department of Hematology/Oncology, University Medical Center Regensburg, Regensburg, Germany; [5]Center for Cellular and Molecular Medicine, Kyushu University Graduate School of Science, Fukuoka, Japan; [6]Institute of Pathology, University Medical Center Regensburg, Regensburg, Germany; [7]Department of Internal Medicine, University of Michigan, Ann Arbor, MI; and [8]Molecular Diagnostics Program, Fred Hutchinson Cancer Research Center, Seattle, WA

There are no plasma biomarkers specific for GVHD of the gastrointestinal (GI) tract, the GVHD target organ most associated with nonrelapse mortality (NRM) following hematopoietic cell transplantation (HCT). Using an unbiased, large-scale, quantitative proteomic discovery approach to identify candidate biomarkers that were increased in plasma from HCT patients with GI GVHD, 74 proteins were increased at least 2-fold; 5 were of GI origin. We validated the lead candidate, REG3α, by ELISA in samples from 1014 HCT patients from 3 transplantation centers. Plasma REG3α concentrations were 3-fold higher in patients at GI GVHD onset than in all other patients and correlated most closely with lower GI GVHD. REG3α concentrations at GVHD onset predicted response to therapy at 4 weeks, 1-year NRM, and 1-year survival ($P \leq .001$). In a multivariate analysis, advanced clinical stage, severe histologic damage, and high REG3α concentrations at GVHD diagnosis independently predicted 1-year NRM, which progressively increased with higher numbers of onset risk factors present: 25% for patients with 0 risk factors to 86% with 3 risk factors present ($P < .001$). REG3α is a plasma biomarker of GI GVHD that can be combined with clinical stage and histologic grade to improve risk stratification of patients. (*Blood.* 2011;118(25): 6702-6708)

Introduction

Acute GVHD, a leading cause of nonrelapse mortality (NRM) after allogeneic hematopoietic cell transplantation (HCT), is measured by dysfunction in 3 organ systems: the skin, liver, and gastrointestinal (GI) tract.[1-4] Acute GVHD of the GI tract affects up to 60% of patients receiving allogeneic HCT,[5,6] causing nausea, vomiting, anorexia, secretory diarrhea, and, in more severe cases, abdominal pain and/or hemorrhage.[7] Acute GVHD typically occurs between 2 and 8 weeks after transplantation, but may occur later,[4] and is often clinically indistinguishable from other causes of GI dysfunction such as conditioning regimen toxicity, infection, or medication. Endoscopic biopsy is often used to confirm the diagnosis,[1,8] but histologic severity on biopsy has not consistently correlated with clinical outcome.[3,8-10] Clinical stage II or greater (> 1 L of diarrhea/d) is associated with reduced survival,[5,6] but daily stool volume can vary considerably. Lower GI GVHD responds poorly to treatment compared with other target organs,[6] and treatment with high-dose systemic steroid therapy carries significant risks, especially infectious complications in profoundly immunosuppressed patients.[11,12] A noninvasive, reliable blood biomarker specific for GVHD of the GI tract would thus significantly aid in the management of patients with this disorder.

Here, we report the discovery and validation of a plasma biomarker of acute GI GVHD: regenerating islet-derived 3-alpha (REG3α), a C-type lectin secreted by Paneth cells.[13,14]

Methods

Proteomic analysis

Methods for sample preparation, protein fractionation, mass spectrometry (MS) analysis, protein identification, and quantitative analysis of protein concentrations during the intact protein analysis system (IPAS) have been previously reported.[15-17]

Patients and samples

Heparinized blood samples were collected weekly for 4 weeks after allogeneic HCT, then monthly for 2 months, and also at the time of key clinical events, including the development of symptoms consistent with GVHD (eg, the onset of diarrhea). Plasma samples were collected prospectively under protocols approved by the University of Michigan Institutional Review Board and stored at the University of Michigan. GVHD assessments, sample processing, and storage were performed as previously described.[7,17] In Regensburg, Germany, and Kyushu, Japan, serum samples were collected weekly and at the onset of GVHD symptoms, prepared, frozen, and stored per institutional guidelines. Samples were shipped and received frozen on dry ice and no sample was thawed more than twice before analysis. REG3α concentrations were stable in samples frozen for at least 5 years. REG3α concentrations of 12 paired healthy donors plasma and serum were similar (mean ± SEM: 20 ± 3 vs 24 ± 3 ng/mL, respectively).

Submitted August 20, 2011; accepted September 27, 2011. Prepublished online as *Blood* First Edition paper, October 6, 2011; DOI 10.1182/blood-2011-08-375006.

*J.L.M.F. and A.C.H. contributed equally to this work.

The online version of this article contains a data supplement.

The publication costs of this article were defrayed in part by page charge payment. Therefore, and solely to indicate this fact, this article is hereby marked "advertisement" in accordance with 18 USC section 1734.

Table 1. Patient characteristics of the University of Michigan validation set

Total, N = 871	GI GVHD*†, N = 167	No GVHD, N = 362	Non-GVHD enteritis‡, N = 52	Skin GVHD, N = 290	*P*
Median age, y (range)	50 (0-67)	46 (0-68)	48 (3-66)	49 (0-70)	.003
Disease, %					.002
Malignant	99 (n = 165)	92 (n = 334)	96 (n = 50)	97 (n = 282)	
Other	1 (n = 2)	8 (n = 28)	4 (n = 2)	3 (n = 8)	
Disease status at transplantation, %§					.63
Other/low/intermediate risk	64 (n = 105)	69 (n = 232)	68 (n = 34)	68 (n = 192)	
High risk	36 (n = 60)	31 (n = 102)	32 (n = 16)	32 (n = 90)	
Donor type, %					< .001
Related donor	45 (n = 75)	64 (n = 233)	54 (n = 28)	40 (n = 115)	
Unrelated donor	55 (n = 92)	36 (n = 129)	46 (n = 24)	60 (n = 175)	
Donor match, %					< .001
Matched donor	70 (n = 117)	90 (n = 325)	92 (n = 48)	73 (n = 212)	
Mismatched donor	30 (n = 50)	10 (n = 37)	8 (n = 4)	27 (n = 78)	
Conditioning regimen intensity, %					.06
High intensity	57 (n = 95)	67 (n = 243)	63 (n = 33)	57 (n = 165)	
Moderate intensity	43 (n = 72)	33 (n = 119)	37 (n = 19)	43 (n = 125)	
Grade of GVHD at onset, %					
0	0 (n = 0)	100 (n = 362)	100 (n = 52)	0 (n = 0)	
I	0 (n = 0)	0 (n = 0)	0 (n = 0)	69 (n = 201)	
Skin stage 1	0 (n = 0)	0 (n = 0)	0 (n = 0)	41 (n = 118)	
Skin stage 2	0 (n = 0)	0 (n = 0)	0 (n = 0)	29 (n = 83)	
II	57 (n = 96)	0 (n = 0)	0 (n = 0)	30 (n = 88)	
Isolated skin stage 3	0 (n = 0)	0 (n = 0)	0 (n = 0)	30 (n = 88)	
Isolated upper GI stage 1†	17 (n = 29)	0 (n = 0)	0 (n = 0)	0 (n = 0)	
Lower GI stage 1†	40 (n = 67)	0 (n = 0)	0 (n = 0)	0 (n = 0)	
III-IV	43 (n = 71)	0 (n = 0)	0 (n = 0)	1 (n = 1)	
Isolated skin stage 4	0 (n = 0)	0 (n = 0)	0 (n = 0)	1 (n = 1)	
GI stage 2†	13 (n = 22)	0 (n = 0)	0 (n = 0)	0 (n = 0)	
GI stage 3†	16 (n = 27)	0 (n = 0)	0 (n = 0)	0 (n = 0)	
GI stage 4†	13 (n = 22)	0 (n = 0)	0 (n = 0)	0 (n = 0)	
Median d after HCT (range)	33 (11-216)	31 (7-185)	24 (7-93)	28 (5-175)	< .001

GI indicates gastrointestinal; HCT, hematopoietic cell transplantation; and CIBMTR, Center for International Blood and Marrow Transplant Research.
*Including 29 patients with isolated upper GI GVHD and 138 with lower ± upper GI GVHD.
†With or without other GVHD target organ involvement.
‡Including 13 patients with isolated upper GI non-GVHD enteritis and 39 patients with lower ± upper GI non-GVHD enteritis.
§High risk of disease status at HCT is according to CIBMTR guidelines.

All patients received pharmacologic GVHD prophylaxis with at least 2 agents, including a calcineurin inhibitor. No donor grafts were depleted of T cells. All patients with available samples were analyzed, including patients who developed other complications of HCT, such as sinusoidal obstruction syndrome (SOS), idiopathic pneumonia syndrome (IPS), and sepsis/bacteremia. Patients were excluded from analysis only if a plasma sample at the time of GVHD onset was not available, or if methylprednisolone > 1 mg/kg (or equivalent) had been administered for > 48 hours at the time of sample acquisition. One sample was analyzed per patient; patients who developed GVHD had samples selected at the time of initial GVHD diagnosis.

The discovery set consisted of plasma samples from 10 HCT patients at the onset of biopsy-proven GI GVHD (clinical stage 1-3) and 10 HCT patients who never developed GVHD and who were matched for key transplantation characteristics (supplemental Table 1, available on the Blood Web site; see the Supplemental Materials link at the top of the online article). Patient samples in the discovery set were not included in the validation set.

The University of Michigan validation set consisted of 4 groups: patients with newly diagnosed GVHD involving the GI tract (with or without other organ involvement; GI GVHD); patients at similar time points who never developed GVHD symptoms (no GVHD); patients with GI distress that was inconsistent with GVHD either by clinical or histologic criteria (non-GVHD enteritis); and patients who presented with isolated skin GVHD (skin GVHD). Patient numbers and characteristics are shown in Table 1. Enteritis was determined to be inconsistent with GVHD on clinical grounds by documentation of infected stool and by resolution of symptoms without steroid treatment. The etiologies of non-GVHD enteritis are listed in Table 2.

Patients from the Regensburg/Kyushu validation set were divided into the same 4 groups; patient characteristics are detailed in supplemental Table 2, with causes of non-GVHD enteritis listed in supplemental Table 3.

Histopathology

GI biopsies were obtained and prepared per institutional guidelines. GVHD was histologically confirmed by duodenal/colonic biopsy in 183 of 197 GI GVHD patients and by skin biopsy in an additional 5 patients with both rash

Table 2. Causes of non-GVHD enteritis in the University of Michigan validation set

Causes of non-GVHD enteritis	% (n)
Non-GVHD lower GI enteritis ± upper GI symptoms: N = 39	
Clostridium difficile infection	54 (21)
Diarrhea with negative biopsy	15 (6)
Nausea/vomiting and diarrhea with negative biopsies	28 (11)
Ulcerative esophagitis and diarrhea (negative biopsies)	3 (1)
Non-GVHD upper GI enteritis without diarrhea (all biopsy negative): N = 13	
Nausea/vomiting	54 (7)
Anorexia	15 (2)
Chemical gastropathy	23 (3)
Helicobacter pylori gastritis	8 (1)

GI indicates gastrointestinal.

and GI symptoms.[9] Skin GVHD was confirmed by biopsy in 272 of 341 patients with rashes and by biopsy of another target organ later affected by GVHD in an additional 8 patients. One hundred sixty-two of 197 patients with GI GVHD had diarrhea. One hundred forty of those 162 patients had biopsies (duodenal = 87, colonic = 53) available for formal grading as described by Lerner.[18] If both duodenal and colonic biopsies were available, colonic biopsies were graded only if duodenal biopsies were negative. We did not impute values for unavailable biopsies.

ELISAs

REG3α ELISA kits were purchased from MBL International (Ab-Match Assembly Human PAP1 kit and Ab-Match Universal kit), and measurements were performed according to the manufacturer's protocol. Samples (diluted 1:10) and standards were run in duplicate, absorbance was measured with a SpectraMax M2 (Molecular Devices), and results were calculated with SoftMax Pro Version 5.4 (Molecular Devices). Elafin, IL2Rα, HGF, TNFR1, and IL-8 ELISAs were performed in duplicate as previously reported.[17,19] Measurements of samples from 66 patients (6.5% of the total population) were repeated in a second ELISA at random intervals and were comparable; correlation coefficient $r = 0.82$, $P < .0001$. Details of the assay parameters are provided in supplemental Table 4.

Statistical analysis

The statistical methods used for the IPAS are as previously described.[15-17] REG3α and albumin concentrations from individual samples in the discovery and validation sets were compared using 2-sample t tests applied to log-transformed concentrations. Differences in characteristics between patient groups were assessed with a Kruskal-Wallis test for continuous values and χ^2 tests of association for categorical values. Receiver operating characteristic (ROC) area under the curves (AUC) were estimated nonparametrically. NRM and relapse mortality were modeled with cumulative incidence regression methods as described by Fine and Gray.[20] One-year overall survival (OS) was modeled with Cox regression methods and probability of response was modeled with logistic regression.

Results

Discovery study

We used a proteomics approach to identify candidate biomarkers in a discovery set of pooled plasma samples taken at similar times after HCT from 10 patients with biopsy-proven GI GVHD and 10 patients without GVHD as previously described (supplemental Table 1).[15-17] We identified and quantified 562 proteins of which 74 were increased at least 2-fold in patients with GVHD (supplemental Table 5). Five proteins (carboxypeptidase N catalytic chain precursor, pancreatic secretory trypsin inhibitor precursor, palladin, lithostathine 1-α precursor, and regenerating islet-derived 3-alpha) were preferentially expressed in the GI tract based on the relevant literature[21-25] and the Human Protein Atlas (http://www.proteinatlas.org/). Commercially available Abs suitable for quantification of plasma concentrations by ELISA were available for only 1 of these 5 proteins, regenerating islet-derived 3-α (REG3α; supplemental Table 5). The MS characteristics of the identified REG3α peptides are shown in supplemental Figure 1 and supplemental Table 6. The plasma concentrations of REG3α in the individual plasma samples in the discovery set were 4 times higher in the patients with GI GVHD than in asymptomatic controls (supplemental Figure 2, $P = .01$).

Validation study

We next evaluated REG3α plasma concentration as a biomarker of GI GVHD in samples from a validation set of 871 allogeneic HCT recipients from the University of Michigan (Table 1). Older transplant recipients, an underlying diagnosis of malignant disease, graft sources from unrelated and HLA-mismatched donors were overrepresented in the groups with GVHD. The median day of sample acquisition for patients with non-GVHD enteritis was closer to the day of transplantation than for all other groups.

Plasma REG3α concentrations were 3 times higher in patients at the onset of GI GVHD than in all other patients, including those with non-GVHD enteritis (Figure 1A). There was no specific cause of non-GVHD diarrhea associated with higher REG3α concentrations. Serum REG3α concentrations were also higher in GI GVHD in an independent validation set of 143 HCT patients from Regensburg, Germany, and Kyushu, Japan, although the absolute values were lower (Figure 1B). This difference may be because of a center effect that depends on several factors, including variations in transplantation conditioning regimens and supportive care; patients receiving high-intensity conditioning regimens had REG3α concentrations that were twice as high as those receiving moderate intensity conditioning, but this difference did not reach statistical significance (Figure 1C). In addition, all patients in Regensburg and Kyushu received oral antibiotics as GVHD prophylaxis, whereas Michigan patients did not and thus increased GI flora might account for greater REG3α secretion.[26] Neither total body irradiation (TBI)–based conditioning nor GVHD prophylaxis regimen significantly impacted REG3α concentrations (data not shown).

We next analyzed REG3α concentrations according to diagnosis and type of GI symptom. In patients with diarrhea caused by GVHD, REG3α concentrations at the onset of GVHD were 5 times higher than in patients with diarrhea from other causes (Figure 1D). In patients without diarrhea, REG3α concentrations were 25% higher when attributable to GVHD compared with other causes, a difference that was not statistically significant.

We measured concentrations of 4 previously reported diagnostic markers of systemic acute GVHD (IL2Rα, TNFR1, IL-8, and HGF),[19] and of elafin, a biomarker for GVHD of the skin,[17] in all patients with diarrhea (Figure 1C, N = 204). ROC curves for these biomarkers distinguished GVHD from non-GVHD with an AUC of 0.80 for REG3α alone and an AUC of 0.81 for a composite panel of all 6 biomarkers (Figure 2). In this analysis, 52% of patients with lower GI GVHD also had skin involvement at onset, and thus the AUC for elafin, which is specific for GVHD of the skin,[17] was greater than expected (supplemental Table 7). ROC curves of REG3α concentrations in patients with diarrhea had similar AUCs in both validation sets (supplemental Figure 3). REG3α was therefore the best single diagnostic biomarker at the onset of symptoms of lower GI GVHD, and additional biomarkers provided no further increased sensitivity or specificity. Using REG3α at the median concentration provided a positive predictive value (PPV) of 95% and a negative predictive value (NPV) of 32% for GVHD as the etiology of diarrhea. Additional predictive values at other REG3α concentrations are provided in supplemental Table 8.

When we categorized patients by the volume of diarrhea, REG3α concentrations at the onset of symptoms continued to distinguish between GVHD and non-GVHD etiologies (Figure 3A, $P < .001$) but did not correlate with the clinical stage of GVHD. Twenty-three of 26 patients with clinical stage IV GI GVHD at onset received full-intensity conditioning, and these patients showed a trend toward higher REG3α concentrations than those with stage 1–3 GI GVHD ($P = .07$; data not shown). Comparing patients who had < 1 L of stool per day because of GVHD versus other causes, the AUC for REG3α was 0.81 (supplemental Figure 4). Plasma REG3α concentrations at the onset of GVHD were significantly

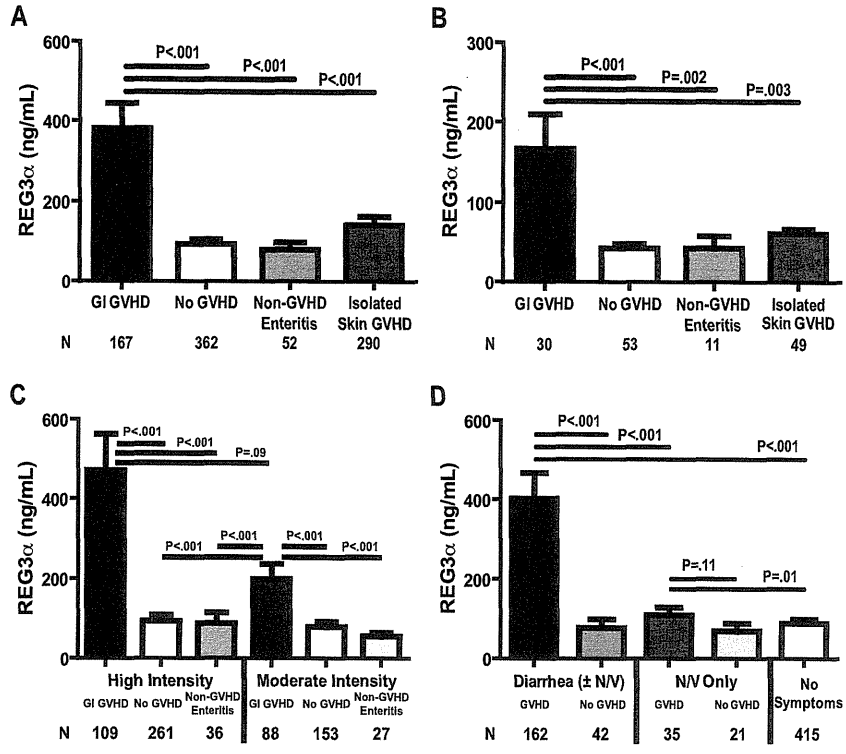

Figure 1. REG3α concentrations in plasma samples from HCT patients of 2 independent validation sets. (A) University of Michigan patients (n = 871). (B) Regensburg, Germany, and Kyushu, Japan (n = 143). (C) Plasma REG3α concentrations in patients classified by GI symptoms and histologic diagnosis and categorized by conditioning regimen intensity. High-intensity regimens included: cyclophosphamide ± cytarabine, thiotepa, fludarabine and/or TBI; cyclophosphamide/VP-16/BCNU; busulfan + cytarabine, clofarabine, melphalan, cyclophosphamide/anasacrin, or cytarabine/cyclophosphamide; BCNU/VP-16/cytarabine/melphalan; TBI ± VP-16; melphalan. Moderate-intensity regimens included: fludarabine + busulfan or treosulfan ± TBI, melphalan, zevalin, or anasacrin/cytarabine; fludarabine ± TBI, melphalan, or cyclophosphamide; fludarabine/BCNU/melphalan; TBI. (D) Patients classified by symptoms and etiology (n = 675).

higher in patients whose GI biopsies showed evidence of severe GVHD with mucosal denudation (histologic grade 4) compared with less severe GVHD (Figure 3B; $P = .03$). Hypoalbuminemia is associated with the protein-losing enteropathy in GI GVHD,[27] and we analyzed the serum albumin level as a potential marker for loss of intravascular proteins into the intestinal lumen. Albumin levels at the onset of GI GVHD also correlated with both the clinical GI GVHD severity (supplemental Figure 5A) and histopathologic severity (supplemental Figure 5B).

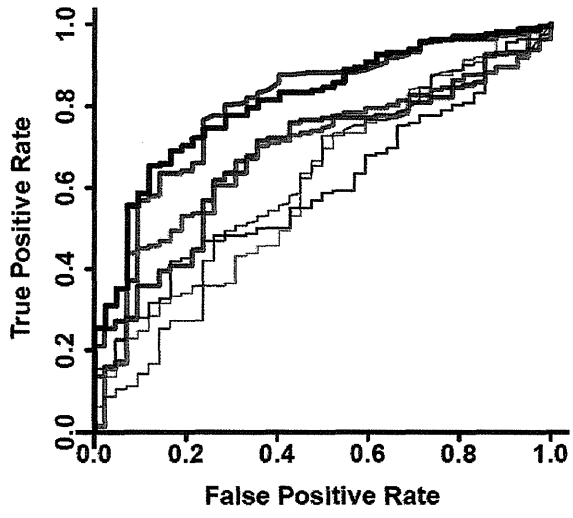

Figure 2. ROC curves for patients with post-HCT diarrhea. ROC curves comparing REG3α concentrations for patients with diarrhea caused by GVHD (n = 162) and not caused by GVHD (N = 42). REGα alone (thick blue): AUC = 0.80; IL2Rα (thick brown): AUC = 0.69; Elafin (thick red): AUC = 0.68; IL-8 (thin blue): AUC = 0.61; HGF (thin brown): AUC = 0.61; TNFR1 (thin red): AUC = 0.60; composite of all 6 biomarkers (solid black): AUC = 0.81.

Prognostic value of REG3α concentrations in patients with lower GI GVHD

The clinical use of any biomarker is greatly enhanced when it provides prognostic information regarding the future status of a disease and/or patient, for example, the likelihood of response to treatment. We therefore evaluated the prognostic significance of REG3α plasma levels in 162 patients taken at the time of diagnosis of lower GI GVHD. REG3α concentrations were 3-fold higher at the time of GVHD diagnosis in patients who had no response to therapy at 4 weeks[28,29] than in patients who experienced a complete or partial response (Figure 4A; $P < .001$)[28,29]; patients responding to therapy still exhibited REG3α concentrations more than twice that of non-GVHD controls. REG3α concentrations at diagnosis also correlated with eventual maximal clinical stage of GI GVHD (supplemental Figure 6); patients presenting with isolated skin GVHD who later developed GI GVHD had concentrations comparable with those with skin GVHD who never developed GI GVHD ($P = .2$; data not shown). Because maximal GVHD grade correlates with NRM,[11] we hypothesized that the REG3α concentration at GVHD diagnosis would also correlate with NRM. We therefore divided the 162 patients into 2 equal groups based on the median REG3α concentration: high (> 151ng/mL, n = 81) and low (≤ 151 ng/mL, N = 81). NRM was twice as high in patients with high REG3α concentrations, and this difference remained significant after adjusting for known risk factors of donor type, degree of HLA match, conditioning intensity, age, and baseline disease severity (59% [95% confidence interval [CI], 48%-69%] vs 34%[95% CI, 24%-46%], $P < .001$, Figure 4B). The incidence of relapse mortality was comparable for both groups (14% [95% CI, 8-24] vs 17% [95% CI, 8-24], $P = .5$; Figure 4C), and thus patients with high REG3α concentrations at the time of GVHD diagnosis experienced significantly inferior 1-year OS (27% [95% CI, 19%-39%] vs 48% [95% CI, 38%-61%], $P = .001$; Figure 4D).